TECHNISCHE UNIVERSITÄT WIEN
Vienna | Austria

DIPLOMARBEIT

Complex scaling for one-dimensional resonance problems in inhomogeneous exterior domains

zur Erlangung des akademischen Grades
Diplom-Ingenieur

im Rahmen des Studiums
Technische Mathematik

unter der Anleitung von
Associate Prof. Dipl.-Math. Dr.rer.nat. Lothar Nannen

eingereicht von
Thomas Heitzinger BSc
Matrikelnummer 01226883

ausgeführt am Institut für Analysis und Scientific Computing
der Fakultät für Mathematik und Geoinformation der Technischen Universität Wien

Wien, 10. September 2018

Unterschrift Verfasser

Unterschrift Betreuer

Abstract

In this thesis the one-dimensional complex scaling method for generalized scaling profiles is introduced and applied to equations of Helmholtz-type with well known solutions in the exterior domain. We discuss the meaning of radiating solutions, prove conditions for the existence of unique radiating solutions to scattering problems, and show that solutions to scaled and unscaled problems are equivalent in some sense. We transfer most of these results to the time-independent Schrödinger equation with quadratically decaying potential functions $V_a(x) = x^2(1 + (x/a)^4)^{-1}$. Potential functions of this type are non-trivial in the exterior domain and lead to solutions with inexplicit asymptotic behavior. We analyze the discrete spectrum of the associated Hamilton operator and test its dependence on the parameter a as well as the influence of discretization parameters. The method is implemented with the finite element software NGSolve.

Danksagung

An erster Stelle gilt mein Dank meinem Betreuer Prof. Dr. Lothar Nannen, der mir beim Verfassen dieser Arbeit mit wertvollem Rat zur Seite gestanden ist und für meine Fragen stets Zeit gehabt hat.

Weiters möchte ich mich bei Freunden und Kollegen bedanken, die meine Studienzeit bereichert haben und insbesondere Michael mit welchem ich in unzähligen Gesprächen mein Wissen erweitern konnte.

Zu guter Letzt bedanke ich mich von ganzem Herzen bei meiner Familie und ausdrücklich meinen Eltern, die mich in den letzten Jahren stets ermutigten und mich in all meinen Entscheidungen unterstützt haben.

Contents

Introduction

We are concerned with the propagation of waves on unbounded domains Ω, which are partitioned into a bounded interior domain Ω_{int} and an unbounded exterior domain Ω_{ext}. For the proper mathematical formulation of such problems, it is essential to pose boundary conditions *at infinity*. Such conditions are referred to as radiation conditions and their function is twofold. In the physical sense, they model asymptotic energy flow away from the origin. Their mathematical purpose is the guarantee for unique solutions.

A common condition for the Helmholtz equation $\Delta u + \omega^2 u = 0$ is the Sommerfeld radiation condition. The disadvantage of this condition is its conditional validity dependent on $\omega > 0$, a constraint that is not met by resonance problems. In some cases the asymptotic properties of solutions are well understood and allow the formulation of a more robust radiation condition in the form of a series representation on the exterior domain. In the absence of such a representation a so called pole condition [HSZ03a; HSZ03b] has been proposed which requires the Laplace transform of solutions in radial direction to have no poles in the lower complex half-plane. In this thesis we will analyze the complex scaling method. It transforms variational formulations on Ω by deforming, or *scaling*, the exterior domain into the complex plane. Under certain conditions it can be shown, that a solution to the unscaled problem is radiating if and only if its holomorphic extension is solution to a complex scaled variational problem. In this sense, the complex scaling method can induce an alternate, but equivalent radiation condition.

When developing numerical methods capable of solving problems on unbounded domains, the problem of discretizing an unbounded domain arises. Some methods are based on the construction of *infinite elements* [HN09] in order to approximate function spaces on the entire unbounded domain. We will focus on a truncation based approach. A characterizing feature of wave functions is their slow decay in space, as is exemplified by the spherical wave functions $u^{\pm}(x) = \frac{\exp(\pm i\omega|x|)}{|x|}$, which are solutions to the Helmholtz equation in three dimensions. This property is significant, as local perturbations have impact over large distances. A discretization method that aims to truncate the unbounded domain to a bounded domain Ω_{int} has to pose a boundary condition on the artificially generated boundary Γ of Ω_{int}. Common conditions of Dirichlet, Neumann or Robin type are not capable of encoding the desired *radiating* condition, and local inaccuracies at the artificial boundary would cause large errors on the entire domain. Some radiation conditions based on series representations in the exterior domain allow the construction of a Dirichlet-to-Neumann, or DtN, operator. Such operators perfectly encode the radiating property at infinity into a local operator on Γ. Boundary conditions of this type are referred to as *transparent* or *absorbing*. The value of DtN operators lies mainly in their analytic application. A numerical implementation is theoretically possible, but infeasible for dimensions larger than one.

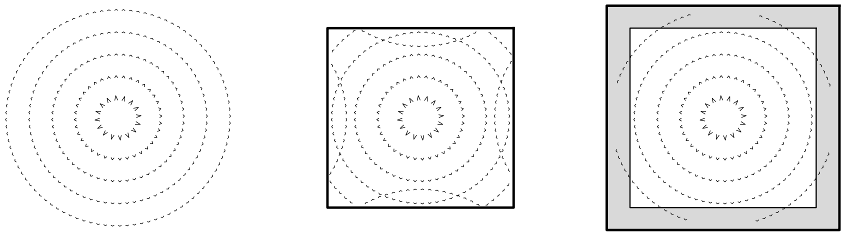

Figure 1: Wave propagation on an unbounded domain *(left)*. Wave propagation on a bounded domain using a reflecting boundary condition *(middle)*. Wave propagation on a bounded domain using an absorbing boundary condition in the form of a perfectly matched layer *(right)*.

The complex scaling method presents a solution to these obstacles, as the core goal of the applied deformation is the construction of a scaled variational formulation that forces its solutions to decay exponentially in radial direction in Ω_{ext}. From a theoretical point of view, this has the advantage of eliminating the need for a DtN operator, whereas numerically it allows for truncation to a bounded domain. The discretized domain consists of the interior domain, which is surrounded by an additional layer called the perfectly matched layer or PML, within which the scaled solution decays exponentially. The boundary condition posed on the exterior boundary of the perfectly matched layer no longer has major impact on the interior domain and can be chosen, for example, as a homogeneous Dirichlet condition. The truncation error introduced by this method is exponentially falling in the thickness of the perfectly matched layer. Hence, the total numerical error is a combination of the standard discretization error and a truncation error. Since a thicker layer increases the computational complexity of the numerical method it is desirable to find a balance between the two.

Implementation

All numerical examples presented in chapter 3 were implemented and executed using the finite element software NGSolve[1], see [Sch14].

Outline of the thesis

The first chapter introduces the complex scaling method. It roughly follows [Nan16] and proves generalizations to some of the stated theorems. However, all considerations are restricted to the one-dimensional case. We discuss the solvability of the complex scaled variational problem and provide conditions under which solutions to scaled and unscaled problems are equivalent in some sense.

In the second chapter we attempt to transfer results previously proven for Helmholtz-type equations to the time-independent Schrödinger equation. Since solutions to the problem on the exterior domain are no longer known explicitly, the treatment of such equations is much more difficult and some asymptotic assumptions have to be made.

[1] https://ngsolve.org

The third chapter consists of numerical tests that aim to demonstrate the practicality of the complex scaling method. We investigate the behavior of the discrete spectrum as a function of the parameter a of the examined potential functions $V_a(x) = x^2(1+(x/a)^4)^{-1}$ and the impact of its poles on our method.

The appendix lists some implications of abstract results proven in the first two chapters.

Chapter 1

Complex scaling

1.1 General

The following two chapters analyze properties of Helmholtz- and Schrödinger-type equations in several variations of weak formulations. The general problem setting can be stated in the form:

$$\text{Find } u \in V : s(u,v) = f(v), \quad v \in V, \tag{1.1.1}$$

for some sesquilinear form s on $V \times V$, linear form f on V and Hilbert space $(V, (\cdot,\cdot)_V)$. We reformulate this problem declaration and define the linear operator $S\colon V \to V$ satisfying $s(u,v) = (Su,v)_V$, $v \in V$ and use the Riesz representation theorem to assign an element $f \in V$ to the functional f, satisfying $f(v) = (f,v)_V$, $v \in V$. Then (1.1.1) is equivalent to

$$Su = f. \tag{1.1.2}$$

A common theme in our treatment of these problems is our pursuit to construct a linear, compact operator K such that $S+K$ is coercive and bounded. It allows the interpretation of $S = (S+K)-K$ as the difference of a coercive, bounded operator $S+K$ and a compact operator K. This representation gives access to the Riesz-Fredholm theory, which in turn allows to draw conclusions about the convergence behavior of discrete eigenvalues and the uniqueness of solutions of some scattering problems (see Appendix / Section B).

The usual application of this method involves the use of a form of Gårdings inequality. Assume $(H, (\cdot,\cdot)_H)$ is another Hilbert space satisfying $V \subset H$ and there exists a compact embedding $E\colon V \to H$. If there are constants $c, \alpha > 0$ such that the Gårding inequality

$$|s(u,u) + c(u,u)_H| \geq \alpha \|u\|_V^2, \quad u \in V,$$

holds, then $K = cE^*E$ and $S = (S + cE^*E) - cE^*E$ is the sought representation of this example. The operator K may also take a more involved form.

1.2 Radiating solutions for equations of Helmholtz-type

Let $\Omega = \mathbb{R}$ be unbounded, $H^1_{\text{loc}}(\mathbb{R})$ be the subspace of $H^1(\mathbb{R})$ containing all locally integrable functions, $H^1_{\text{comp}}(\mathbb{R})$ the subspace of $H^1(\mathbb{R})$ containing all functions f with

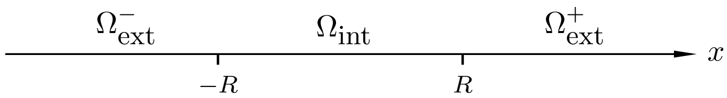

Figure 1.1: The decomposition of $\mathbb{R}$.

compact support $\operatorname{supp} f := \overline{\{ x \in \Omega : f(x) \neq 0 \}}$ and $L^\infty(\mathbb{R})$ the space of essentially bounded functions. For a fixed parameter $R > 0$ we split $\mathbb{R}$ into the interior space $\Omega_{\text{int}} = (-R, R)$ and the exterior space $\Omega_{\text{ext}} = (-\infty, -R] \cup [R, \infty)$. We further pose the restrictions $p \in L^\infty(\Omega), g \in L^2(\Omega)$ and $\operatorname{supp} p, \operatorname{supp} g \subset \Omega_{\text{int}}$.

For values $\omega \in \mathbb{C}$, $\Re[\omega] > 0$ we are interested in solutions $u \in H^2_{\text{loc}}(\Omega)$ of the scattering problem

$$-u''(x) - \omega^2 \left(1 + p(x)\right) u(x) = g(x), \quad x \in \Omega, \tag{1.2.1}$$

$$u \text{ is radiating for } |x| \to \infty. \tag{1.2.2}$$

Condition (1.2.2) should pose two restrictions on solutions of (1.2.1): Uniqueness and physical sensibility. The latter is essentially a constraint on the energy flow J through $\Gamma = \overline{\Omega_{\text{int}}} \cap \overline{\Omega_{\text{ext}}}$

$$J_\Gamma(u) = -\frac{1}{2\omega} \Im[\int_\Gamma u \frac{\partial \overline{u}}{\partial n} \, \mathrm{d}s], \tag{1.2.3}$$

where n is the outer normal vector of Ω_{int}. Since we are solely interested in sources located in the interior Ω_{int}, the energy flow should be non-negative. Unfortunately this constraint is not sufficiently restrictive to achieve uniqueness. Let $u_{\text{ext}} := u|_{\Omega_{\text{ext}}}$, then (1.2.1) restricted to Ω_{ext} reduces to the Helmholtz equation

$$-u''_{\text{ext}} - \omega^2 u_{\text{ext}} = 0, \quad x \in \Omega_{\text{ext}}, \tag{1.2.4}$$

and can be solved easily. The exterior domain consists of the two sections $\Omega_{\text{ext}}^- := \Omega_{\text{ext}} \cap \mathbb{R}_{\leq 0}$ and $\Omega_{\text{ext}}^+ := \Omega_{\text{ext}} \cap \mathbb{R}_{\geq 0}$. For $x \in \Omega_{\text{ext}}^+$ and $\omega \neq 0$ the general solution of the Helmholtz equation is given by

$$C_1 \exp(i\omega(x - R)) + C_2 \exp(-i\omega(x - R)), \quad C_1, C_2 \in \mathbb{C}. \tag{1.2.5}$$

Here, the energy flow through the partial boundary $\overline{\Omega_{\text{int}}} \cap \overline{\Omega_{\text{ext}}^+} = \{R\}$ is $J_{\{R\}}(u_{\text{ext}}) = {}^{(|C_1|^2 - |C_2|^2)}/_2$. Although this restriction does not yield a unique solution, it is clear that $\exp(-i\omega(x - R))$ is responsible for negative energy flow. Therefore we will require $C_2 = 0$ for $x \in \Omega_{\text{ext}}^+$ and through analog reasoning $C_1 = 0$ for $x \in \Omega_{\text{ext}}^-$. We are now able to formulate a radiation condition for equations of Helmholtz-type.

Definition 1.2.1. *(Radiation condition (1.2.2)) A solution u of (1.2.4) is said to be radiating, if and only if u_{ext} is of the form*

$$u_{ext}(x) = \begin{cases} C_1 \exp(i\omega(x - R)), & x \in \Omega_{ext}^+ \\ C_2 \exp(-i\omega(x + R)), & x \in \Omega_{ext}^- \end{cases},$$

for some $C_1, C_2 \in \mathbb{C}$.

For given boundary values u_0^+, u_0^- the exterior problem

$$\begin{aligned} -u''_{\text{ext}} - \omega^2 u_{\text{ext}} &= 0, \quad x \in \Omega_{\text{ext}}, \\ u_{\text{ext}}(\pm R) &= u_0^\pm, \\ u_{\text{ext}} &\text{ is radiating,} \end{aligned}$$

has a unique solution and allows the definition of unique, continuous and linear Dirichlet-to-Neumann operators $\mathrm{DtN}_\pm^\omega \colon \mathbb{C} \to \mathbb{C}$ as

$$\mathrm{DtN}_+^\omega[u_0^+] \coloneqq u'_{\text{ext}}(u_0^+) \quad \text{and} \quad \mathrm{DtN}_-^\omega[u_0^-] \coloneqq -u'_{\text{ext}}(u_0^-).$$

Note, that the evaluation of these operators simplifies to $\mathrm{DtN}_\pm^\omega[u_0^\pm] = i\omega u_{\text{ext}}(u_0^\pm)$. If the dependence on ω is inconsequential, we will omit the argument and write $\mathrm{DtN}_\pm$ instead of $\mathrm{DtN}_\pm^\omega$. We multiply (1.2.1) with test functions $v \in H^1(\Omega_{\text{int}})$ and integrate on the interior domain. For $u_{\text{int}} \coloneqq u|_{\Omega_{\text{int}}}$ we use the Dirichlet-to-Neumann operators and partial integration to get

$$\begin{aligned} \int_{\Omega_{\text{int}}} \left(-u''_{\text{int}}\overline{v} - \omega^2(1+p)u_{\text{int}}\overline{v}\right) \mathrm{d}x = \int_{\Omega_{\text{int}}} &\left(u'_{\text{int}}\overline{v}' - \omega^2(1+p)u_{\text{int}}\overline{v}\right) \mathrm{d}x \\ &+ \mathrm{DtN}_-[u(-R)]\overline{v(-R)} - \mathrm{DtN}_+[u(R)]\overline{v(R)}, \end{aligned}$$

and similarly on the exterior domain with $v \in H^1_{\text{comp}}(\Omega_{\text{int}})$

$$\int_{\Omega^\pm_{\text{ext}}} \left(-u''_{\text{ext}}\overline{v} - \omega^2 u_{\text{ext}}\overline{v}\right) \mathrm{d}x = \int_{\Omega^\pm_{\text{ext}}} \left(u'_{\text{ext}}\overline{v}' - \omega^2 u_{\text{ext}}\overline{v}\right) \mathrm{d}x \pm \mathrm{DtN}_\pm[u(\pm R)]\overline{v(\pm R)}.$$

We arrive at a weak formulations for the interior problem:

$$\text{Find } u_{\text{int}} \in H^1(\Omega_{\text{int}}) : s_\omega(u_{\text{int}}, v) = f(v), \quad v \in H^1(\Omega), \tag{1.2.6}$$

where

$$\begin{aligned} s_\omega(u_{\text{int}}, v) &\coloneqq \int_{\Omega_{\text{int}}} \left(u'_{\text{int}}\overline{v}' - \omega^2(1+p)u_{\text{int}}\overline{v}\right) \mathrm{d}x \\ &\quad + \mathrm{DtN}_-[u_{\text{int}}(-R)]\overline{v(-R)} - \mathrm{DtN}_+[u_{\text{int}}(R)]\overline{v(R)}, \\ f(v) &\coloneqq \int_{\Omega_{\text{int}}} gv \, \mathrm{d}x. \end{aligned}$$

and a formulation for the exterior problem:

$$\text{Find } u_{\text{ext}} \in H^1_{\text{loc}}(\Omega_{\text{ext}}) : \int_{\Omega^\pm_{\text{ext}}} \left(u'_{\text{ext}}\overline{v}' - \omega^2 u_{\text{ext}}\overline{v}\right) \mathrm{d}x = \mp \mathrm{DtN}_\pm[u_{\text{ext}}(\pm R)]\overline{v(\pm R)}, \tag{1.2.7}$$

for all $v \in H^1_{\text{comp}}(\Omega_{\text{ext}})$ under the continuity constraints $u_{\text{int}}(\pm R) = u_{\text{ext}}(\pm R)$. It is convenient to pose (1.2.6) and (1.2.7) as a combined weak formulation on $\mathbb{R}$ as:

$$\text{Find } u \in H^1_{\text{loc}}(\mathbb{R}) : \int_{\mathbb{R}} \left(u'\overline{v}' - \omega^2(1+p)u\overline{v}\right) \mathrm{d}x = \int_{\mathbb{R}} gv \, \mathrm{d}x, \quad v \in H^1_{\text{comp}}(\mathbb{R}). \tag{1.2.8}$$

Since the boundary terms of s_ω are scalar, we write $\mathrm{Tr}_R \colon \Omega_{\text{int}} \to \mathbb{C}$ to denote continuous (and compact) point evaluation at the point R (see A.1), whereas in higher dimensions the use of the trace operator $\mathrm{Tr} \colon H^1(\Omega) \to L^2(\partial\Omega)$ (see A.2) would be appropriate. In order to prove the continuity of s_ω we first reinterpret the boundary terms as follows (we only demonstrate treatment of the term at R and omit the brackets of DtN if convenient):

$$\begin{aligned}\mathrm{DtN}_+[u_{\mathrm{int}}(R)]\overline{v(R)} &= (\mathrm{DtN}_+[u_{\mathrm{int}}(R)], v(R))_{\mathbb{C}} \\ &= (\mathrm{DtN}_+ \, \mathrm{Tr}_R u_{\mathrm{int}}, \mathrm{Tr}_R v)_{\mathbb{C}} \\ &= (\mathrm{Tr}_R^* \, \mathrm{DtN}_+ \, \mathrm{Tr}_R u_{\mathrm{int}}, v)_{H^1(\Omega_{\mathrm{int}})}.\end{aligned}$$

It is now easy to see that the sesquilinear form s_ω is continuous on $H^1(\Omega_{\mathrm{int}})\times H^1(\Omega_{\mathrm{int}})$, as a result of the boundedness of p and continuity of the operator $(\mathrm{Tr}_R^* \, \mathrm{DtN}_+ \, \mathrm{Tr}_R) : H^1(\Omega_{\mathrm{int}}) \to H^1(\Omega_{\mathrm{int}})$. Let E be the compact embedding $\mathrm{E} : H^1(\Omega_{\mathrm{int}}) \to L^2(\Omega_{\mathrm{int}})$ (see A.4), then we are able to define the operator $\mathrm{K} : H^1(\Omega_{\mathrm{int}}) \to H^1(\Omega_{\mathrm{int}})$ as

$$\mathrm{K}(\omega) := C(\omega)\mathrm{E}^\star\mathrm{E} + \left(\mathrm{Tr}_{-R}^\star \, \mathrm{DtN}_- \, \mathrm{Tr}_{-R} + \mathrm{Tr}_R^\star \, \mathrm{DtN}_+ \, \mathrm{Tr}_R\right),$$

with $C(\omega) = 1 + |\omega|^2 \left(1 + \|p\|_{L^\infty(\Omega_{\mathrm{int}})}\right)$. It is compact and s_ω satisfies the Gårding inequality

$$\left|s_\omega(v_{\mathrm{int}}, v_{\mathrm{int}}) + (K(\omega)v_{\mathrm{int}}, v_{\mathrm{int}})_{H^1(\Omega_{\mathrm{int}})}\right| \geq \|v_{\mathrm{int}}\|^2_{H^1(\Omega_{\mathrm{int}})}. \tag{1.2.9}$$

This estimation already gives full insight into the existence of unique radiating solutions of the weak scattering problem (1.2.8).

Definition 1.2.2. *(Resonances to scattering problem (1.2.1)) Let $\Omega = \mathbb{R}$, $u \in H^1_{loc} \setminus \{0\}$ and $\Re[\omega] > 0$. If (u, ω) solves the problem*

$$\begin{aligned} -u''(x) = \omega^2(1 + p(x))u(x) \quad &, x \in \Omega, \\ &u \textit{ is radiating,}\end{aligned} \tag{1.2.10}$$

then ω is said to be a resonance to the scattering problem (1.2.1).

Corollary 1.2.3. *(to Appendix / Theorem B.1) The weak scattering problem (1.2.8) has a unique solution if and only if ω is not a resonance. Radiating solutions are of the form*

$$u(x) = \begin{cases} u_{int}(-R)\exp(-i\omega(x-R)), & x \in \Omega^-_{ext} \\ u_{int}(x), & x \in \Omega_{int} \\ u_{int}(R)\exp(i\omega(x-R)), & x \in \Omega^+_{ext} \end{cases}, \tag{1.2.11}$$

where $u_{int} \in H^1(\Omega_{int})$ is a solution to (1.2.6).

1.3 Complex scaled variables

Although the numerical implementation of DtN operators in one dimension is straightforward, their use in higher dimensions becomes impractical, since an analogous construction of radiation condition 1.2.1 in higher dimensions is usually stated in the form of an infinite series. Additionally, the dependence of DtN operators on ω would be a hindrance in the numerical treatment of resonance problems, as it would lead to a nonlinear system of equations. The complex scaling method avoids these issues by treating variational formulations on the entire unbounded domain Ω.

Definition 1.3.1. *(Deformation function) We refer to a function* $\tau\colon \mathbb{R}_{\geq 0} \to \mathbb{R}_{\geq 0}$ *as a deformation function if it is twice differentiable and satisfies the conditions*

(i) $\tau(0) = 0$.

(ii) $\tau'(x) > 0$ *for* $x > 0$.

(iii) $\liminf_{x\to\infty} \tau'(x) > 0$.

Deformation functions serve as an important component in the introduction of complex scaled variables. For any deformation function τ and scaling parameter $\alpha > 0$ we can define the complex scaling function $\gamma\colon \mathbb{R}_{\geq 0} \to \mathbb{C}$ as

$$\gamma_{\tau,\alpha,R}(r) \coloneqq \begin{cases} r, & r \in [0, R] \\ r + i\alpha\tau(r - R), & r \geq R \end{cases}, \tag{1.3.1}$$

along with the corresponding complex scaled variable

$$x_\gamma(x) \coloneqq \operatorname{sgn}(x)\gamma_{\tau,\alpha,R}(|x|). \tag{1.3.2}$$

The complex scaled variable is continuous on its entire domain and inherits the regularity of τ for all $x \in \mathbb{R} \setminus \{-R, R\}$. Last, we introduce the complex scaled function

$$u_\gamma \coloneqq u \circ x_\gamma. \tag{1.3.3}$$

Remark 1.3.2. *Solutions* u *of (1.2.8) are functions on* $\mathbb{R}$*, and as such the composition* $u \circ x_\gamma$ *with the complex valued variable* x_γ *is not well defined on* Ω_{ext}*. We can resolve this problem by extending* u_{ext} *to* $\Omega_{ext}^{\mathbb{C}} \coloneqq \{\, z \in \mathbb{C} : \Re[z] \in \Omega_{ext} \,\}$*. Solution representation (1.2.11) shows that the restrictions* $u_{ext}|_{\Omega_{ext}^+}$ *and* $u_{ext}|_{\Omega_{ext}^-}$ *are holomorphic functions. According to the identity theorem, there exists a unique holomorphic extension* $u_{ext}^{\mathbb{C}}$ *onto* $\Omega_{ext}^{\mathbb{C}}$ *satisfying* $u_{ext}^{\mathbb{C}}|_{\Omega_{ext}} = u_{ext}$*. In order to improve legibility, we will continue to write* $u \circ x_\gamma$ *with the understanding that the extension of* u *is used whenever necessary. Since* x_γ *is continuous and differentiable for all* $x > R$*, there holds* $u_\gamma \in H^1_{loc}(\mathbb{R})$*.*

Definition 1.3.3. *(Critical region of a complex scaled variable) Each complex scaled variable* x_γ *induces a critical region*

$$\operatorname{crit} x_\gamma \coloneqq \operatorname{crit}_+ x_\gamma \cup \operatorname{crit}_- x_\gamma, \tag{1.3.4}$$

where

$$\operatorname{crit}_+ x_\gamma \coloneqq \Big\{\, z \in \mathbb{C} : \Im[z] \in \Big(0, \Im\big[x_\gamma(\Re[z])\,\big]\Big) \,\Big\} \text{ and}$$
$$\operatorname{crit}_- x_\gamma \coloneqq \Big\{\, z \in \mathbb{C} : \Im[z] \in \Big(\Im\big[x_\gamma(\Re[z])\,\big], 0\Big) \,\Big\}.$$

The importance of the critical region (see Figure 1.2) of complex scaled variables will become apparent in chapter 2.

1.4 Analysis of scaled solutions

1.4.1 Preparations

The introduction of complex scaled functions leads us to a generalized scaled variational formulation which we will motivate as follows: Assume u solves the Helmholtz equation

$$-u'' - \omega^2 u = 0, \quad x \in \Omega.$$

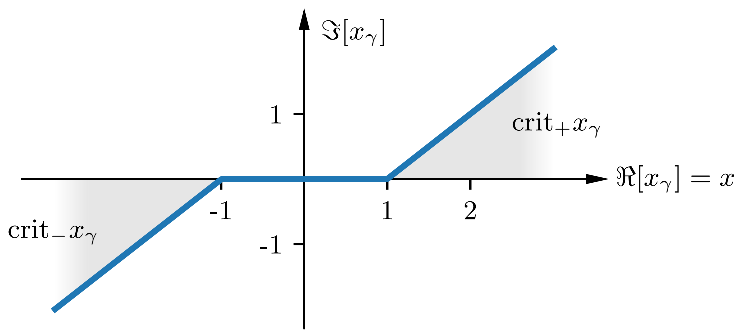

Figure 1.2: An example of a complex scaled variable with parameters $\tau(r) = r, \alpha = 1$ and $R = 1$.

After some careful consideration, we can see that the complex scaled counterpart u_γ of such solutions solves the scaled equation

$$-\left(\frac{u_\gamma'}{x_\gamma'}\right)' - \omega^2 x_\gamma' u_\gamma = 0, \quad x \in \Omega,$$

where the terms x_γ' and $1/x_\gamma'$ can be interpreted as *weights*. The same weights can be found in (1.4.1).

The following sections will deal with a generalized sesquilinear form

$$\begin{aligned} s_\gamma(u,v) &= a(u,v) - b(u,v), \\ a(u,v) &:= \int_{\mathbb{R}} \frac{1}{x_\gamma'(x)} u'(x)\overline{v'(x)}\,\mathrm{d}x, \\ b(u,v) &:= \int_{\mathbb{R}} \rho_\gamma(x) x_\gamma'(x) u(x)\overline{v(x)}\,\mathrm{d}x, \end{aligned} \tag{1.4.1}$$

which operates on some yet to be determined Hilbert space. If $\rho(x) = \omega^2(1 + p(x))$ then (1.4.1) acts as a scaled form for equations of Helmholtz-type. Other functions ρ will be used in chapter 2 to proof results for the time-independent Schrödinger equation.

Definition 1.4.1. *(Inequality modulo constant) The symbol $\preceq$ is used to express inequality modulo constant, or more specifically $a \preceq_\theta b$ if and only if there exists some $C > 0$ independent of θ such that $a \leq Cb$. We will usually simply write $\preceq$ instead of $\preceq_\theta$ if the parameter θ is clear from context, or otherwise clarify it beforehand. Similarly we write $b \succeq a$ if and only if $a \preceq b$.*

Proposition 1.4.2. *Let $I \subset \mathbb{R}$ and $f\colon I \to \mathbb{C}$. If there exists a fixed $\theta \in \mathbb{R}$ and $\varepsilon > 0$ such that $\arg(f(x)) \in [\theta - (\frac{\pi}{2} - \varepsilon), \theta + (\frac{\pi}{2} - \varepsilon)]$ for all $x \in I$, then there holds*

$$\Re[\exp(-i\theta)f(x)] \succeq |f(x)|\,, \quad x \in I. \tag{1.4.2}$$

Proof.

$$\begin{aligned} \Re[\exp(-i\theta)f(x)] &= |f(x)|\,\Re\Big[\exp\Big(i\left(\arg(f(x)) - \theta\right)\Big)\Big] \\ &= |f(x)| \cos\Big(\arg(f(x)) - \theta\Big) \\ &\geq |f(x)| \cos\left(\frac{\pi}{2} - \varepsilon\right). \end{aligned}$$

□

1.4.2 Weighted Sobolev spaces

Unfortunately, in the standard norm $\|\cdot\|_{H^1(\mathbb{R})}$ the sesquilinear form $s_\gamma(\cdot,\cdot)$ defined in (1.4.1) is neither continuous nor does it adhere to a Gårding inequality of the form $\left|s(u,u)+C_1(u,u)_{L^2([-C_3,C_3])}\right| \geq C_2\|u\|^2_{H^1(\mathbb{R})}$ for some $C_1, C_2, C_3 > 0$. The following example illustrates these issues in a simplified setting.

Example 1.4.3. *Let $\Omega_{int} = [-1,1]$, $\Omega_{ext} = \mathbb{R}\setminus\Omega_{int}$ and observe the weak formulation of the complex scaled Helmholtz-type equation with parameters $p(x) = \mathbb{1}_{\Omega_{int}}(x)$ and $\omega = 1$. The deformation function is quadratic $\tau(r) = r^2$ with scaling constant $\alpha = 1$. Under these circumstances, the sesquilinear form of interest becomes*

$$s(u,v) = \int_{\mathbb{R}} \left(\frac{1}{x'_\gamma} u'\overline{v'} - x'_\gamma(1+p)u\overline{v}\right) \mathrm{d}x,$$

with $x'_\gamma = 1$ for $x \in \Omega_{int}$ and $x'_\gamma = 1 + i2(x-1)$ otherwise.

To show that $s(\cdot,\cdot)$ is not continuous on $H^1(\mathbb{R}) \times H^1(\mathbb{R})$ we define $(\varphi_k)_{k\in\mathbb{Z}}$ as $\varphi_k(x) \coloneqq \delta_{k,x} + \delta_{k+1,x}$ for $x \in \mathbb{Z}$, and linearly interpolated otherwise. Since all φ_k are piecewise linear, continuous and $\operatorname{supp}\varphi_k = [k-1, k+2]$ is bounded, these functions lie in $H^1(\mathbb{R})$. We further observe that $\operatorname{supp}\varphi'_k = [k-1,k] \cup [k+1,k+2]$ and consequently $\varphi'_k\varphi'_{k+1} = 0$. For $k > 2$ we can estimate

$$\begin{aligned}
\left|s(\varphi_k,\varphi_{k+1})\right| &= \left|\int_{\mathbb{R}} x'_\gamma(1+p)\varphi_k\varphi_{k+1}\,\mathrm{d}x\right| \\
&\geq \int_{k-1}^{k+2} \Im\left[x'_\gamma(1+p)\varphi_k\varphi_{k+1}\right]\mathrm{d}x \\
&\geq 2(k-2)\int_{k-1}^{k+2} \varphi_k\varphi_{k+1}\,\mathrm{d}x.
\end{aligned}$$

If we assume that $s(\cdot,\cdot)$ is continuous, then there exists a constant $C > 0$ such that

$$2(k-2)\int_{k-1}^{k+2} \varphi_k\varphi_{k+1}\,\mathrm{d}x \leq \left|s(\varphi_k,\varphi_{k+1})\right| \leq C\|\varphi_k\|_{H^1(\mathbb{R})}\|\varphi_{k+1}\|_{H^1(\mathbb{R})}.$$

Since both $\int_{k-1}^{k+2}\varphi_k\varphi_{k+1}\,\mathrm{d}x$ and $\|\varphi_k\|_{H^1(\mathbb{R})}\|\varphi_{k+1}\|_{H^1(\mathbb{R})}$ are strictly positive and constant in k, the assumption must be wrong.

Similarly, we can construct a counterexample to show that a form of Gårdings inequality cannot hold. To do so, we define the sequence $(\psi_k)_{k\in\mathbb{N}}$ (see Figure 1.3), starting with $\psi_1(x) \coloneqq \delta_{x,1}$ for $x \in \mathbb{Z}$ and linearly interpolated otherwise. For $k \geq 2$ we set

$$\psi_k(x) \coloneqq \begin{cases} \frac{1}{k^2}\psi_1\left(k^2 x \mod 2\right), & x \in [k-1,k+1] \\ 0, & \text{otherwise} \end{cases}.$$

These functions have the properties $\left|\psi_k(x)\right| \leq 1/k^2$ and $\left|\psi'_k(x)\right| = 1$ for $x \in [k-1, k+1]$ and are both zero otherwise. If we assume that the Gårding inequality $\left|s(u,u)+C_1(u,u)_{L^2([-C_3,C_3])}\right| \geq C_2\|u\|^2_{H^1(\mathbb{R})}$ holds for some constants $C_1, C_2, C_3 > 0$ and all $u \in H^1(\mathbb{R})$, then we get

$$\begin{aligned}
C_2\int_{\mathbb{R}}\left(\psi_k^2 + \psi_k'^2\right)\mathrm{d}x &\leq \left|\int_{-C_3}^{C_3} C_1\psi_k^2\,\mathrm{d}x + \int_{\mathbb{R}}\left(\left(-x'_\gamma(1+p)\right)\psi_k^2 + \frac{1}{x'_\gamma}\psi_k'^2\right)\mathrm{d}x\right| \\
&\leq \int_{\mathbb{R}}\left(\left|C_1\mathbb{1}_{[-C_3,C_3]} - x'_\gamma(1+p)\right|\psi_k^2 + \frac{1}{|x'_\gamma|}\psi_k'^2\right)\mathrm{d}x,
\end{aligned}$$

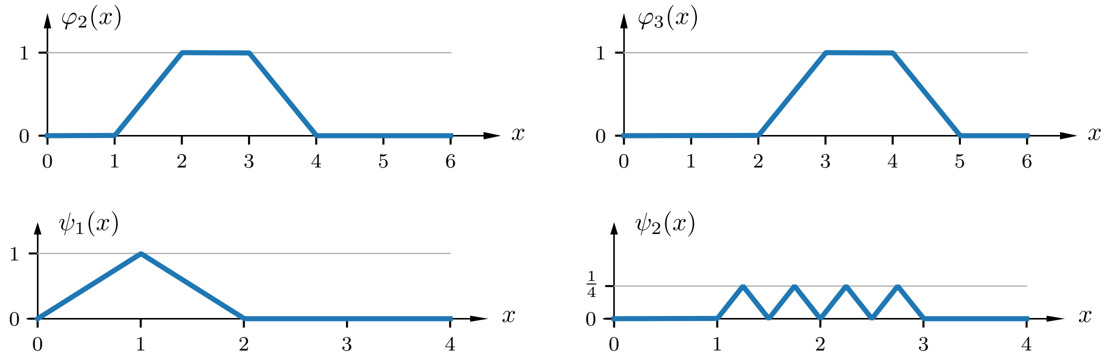

Figure 1.3: Some of the functions used in the counterexamples for continuity and the Gårding inequality with respect to $H^1(\mathbb{R})$.

or equivalently for k large enough such that $|x_\gamma'(k-1)| \geq {}^2\!/\!{}_{C_2}$

$$\begin{aligned}0 &\leq \int_{\mathbb{R}} \left(\left|C_1 \mathbb{1}_{[-C_3,C_3]} - x_\gamma'(1+p)\right| - C_2\right) \psi_k^2 \,\mathrm{d}x + \int_{\mathbb{R}} \left(\frac{1}{|x_\gamma'|} - C_2\right) \psi_k'^2 \,\mathrm{d}x \\ &\leq \int_{k-1}^{k+1} |\mathcal{O}(x)| \frac{1}{k^2} \,\mathrm{d}x + \int_{k-1}^{k+1} \left(\frac{C_2}{2} - C_2\right) \mathrm{d}x \\ &\leq \mathcal{O}\left({}^1\!/\!{}_k\right) - C_2,\end{aligned}$$

which cannot hold for all k. //

To circumvent these problems we will construct Sobolev spaces that are tailored to our needs.

Definition 1.4.4. *(Weight function) We call w a weight function on Ω, if it is an almost everywhere positive, measurable function mapping Ω to $\mathbb{R}$.*

Weight functions usually occur in sets and we will write $\boldsymbol{w}$ to express a set

$$\boldsymbol{w} = \{\, w_\alpha : |\alpha| \leq k \,\},$$

for some $k \in \mathbb{N}$ and multiindices α.

Definition 1.4.5. *(Weighted L^p spaces) Let $1 \leq p \leq \infty$ and w a weight function, then the weighted L^p space on Ω with respect to weight function w, denoted $L^p(\Omega, w)$, is the space of all measurable functions u such that*

$$\|u\|_{L^p(\Omega,w)} = \left(\int_\Omega |u(x)|^p \, w(x) \,\mathrm{d}x\right)^{1/p} < \infty,$$

if $p < \infty$ and

$$\|u\|_{L^p(\Omega,w)} = \operatorname*{ess\,sup}_{x\in\Omega}(w(x)u(x)) < \infty$$

otherwise.

Definition 1.4.6. *(Weighted Sobolev space) The weighted Sobolev space $H^k(\Omega, \boldsymbol{w})$ is the space of all functions $L^2(\Omega, w_0)$, such that*

$$\|u\|_{H^k(\Omega,\boldsymbol{w})} = \left(\sum_{|\alpha|\leq k} \int_\Omega \left(\mathrm{D}^\alpha u(x)\right)^2 w_\alpha(x) \,\mathrm{d}x\right)^{1/2} < \infty.$$

Theorem 1.4.7. *Let $w_\alpha^{-1} \in L^1_{loc}(\Omega)$ for all $w_\alpha \in \boldsymbol{w}$, then the space $H^k(\Omega, \boldsymbol{w})$ forms a Hilbert space.*

Proof. See [Fau09], Theorem 3.3. □

Each complex scaled variable x_γ allows the definition of an associated Hilbert space $H^1_\gamma(\mathbb{R})$ with weight functions $(w_0, w_1) := (|x'_\gamma|, |1/x'_\gamma|)$. Since x'_γ has a constant real part of 1 and τ' is continuous, we see that both $|x'_\gamma|$ and $|1/x'_\gamma|$ are positive and continuous. Hence, they are valid weight functions and elements of $L^1_{\text{loc}}(\mathbb{R})$. We define $H^1_\gamma(\mathbb{R}) := H^1(\mathbb{R}, \{w_0, w_1\})$ and are able to employ theorem 1.4.7 which states that $H^1_\gamma(\mathbb{R})$ is indeed a Hilbert space as initially claimed and its inner product is given by

$$(u, v)_{H^1_\gamma(\mathbb{R})} := \int_{\mathbb{R}} \left(|1/x'_\gamma| \, u'(x)\overline{v'(x)} + |x'_\gamma| \, u(x)\overline{v(x)} \right) \mathrm{d}x.$$

Theorem 1.4.8. *If there exists $c > 0$ such that $w_\alpha(x) \geq c$ holds almost everywhere in Ω, then $H^k(\Omega, \boldsymbol{w})$ continuously embeds into $H^k(\Omega)$.*

Proof. See [Fau09], Theorem 3.21. □

Remark 1.4.9. *For any bounded subset A of $\mathbb{R}$ the weight functions $(w_0, w_1) = (|x'_\gamma|, |1/x'_\gamma|)$ satisfy the requirement of the previous theorem. Together with Theorem A.4 we see that $H^1_\gamma(A)$ is compactly embedded in $L^2(A)$.*

We have finally finished all preparations. The constructed Sobolev spaces will prove their utility in the next section.

1.4.3 Uniqueness of scaled solutions

The following theorem makes statements for $s_\gamma(\cdot, \cdot)$ which are very similar to the properties of $s_\omega(\cdot, \cdot)$ shown in section 1.2 – we will prove continuity and a form of Gårdings inequality. The main differences, apart from a more involved argument, are s_γ acting on the unbounded domain $\Omega = \mathbb{R}$ and the use of a different compact perturbation in the Gårding inequality.

Theorem 1.4.10. *Let τ be a deformation function and $\alpha > 0$. Furthermore, let the function $\rho : \mathbb{C} \to \mathbb{C}$ be holomorphic in the critical region of x_γ, bounded in Ω_{int} and satisfying $\rho_\gamma(x) := (\rho \circ x_\gamma)(x) \to \rho_0$ for $|x| \to \infty$ and $\rho_0 \in \mathbb{C}$. Last, let $s_\gamma(u, v) = a(u, v) - b(u, v)$ be composed of the two sesquilinear forms*

$$a(u, v) = \int_{\mathbb{R}} \frac{1}{x'_\gamma(x)} u'(x)\overline{v'(x)} \, \mathrm{d}x,$$
$$b(u, v) = \int_{\mathbb{R}} \rho_\gamma(x) x'_\gamma(x) u(x)\overline{v(x)} \, \mathrm{d}x,$$

and $\| \cdot \|_{H^1_\gamma(\mathbb{R})}$ the weighted Sobolev norm associated with the complex scaled variable x_γ arising from τ and α.

If there exists $\widetilde{R} > R$ and $\phi \in (0, \pi)$ such that $\arg(\rho_\gamma(x)x'_\gamma(x)) \in [\phi, \phi + \frac{\pi}{2}]$ and $|\rho_\gamma(x)| \geq \frac{|\rho_0|}{2}$ for all $|x| \geq \widetilde{R}$, then the sesquilinear form s_γ is continuous on $H^1_\gamma(\mathbb{R}) \times H^1_\gamma(\mathbb{R})$ and satisfies a Gårding inequality:

$$|s_\gamma(u, v)| \preceq \|u\|_{H^1_\gamma(\mathbb{R})} \|v\|_{H^1_\gamma(\mathbb{R})}, \qquad u, v \in H^1_\gamma(\mathbb{R}), \tag{1.4.3}$$

$$\left| s_\gamma(u, u) + C(u, u)_{L^2([-\widetilde{R}, \widetilde{R}])} \right| \succeq \|u\|^2_{H^1_\gamma(\mathbb{R})}, \qquad u, \in H^1_\gamma(\mathbb{R}), \tag{1.4.4}$$

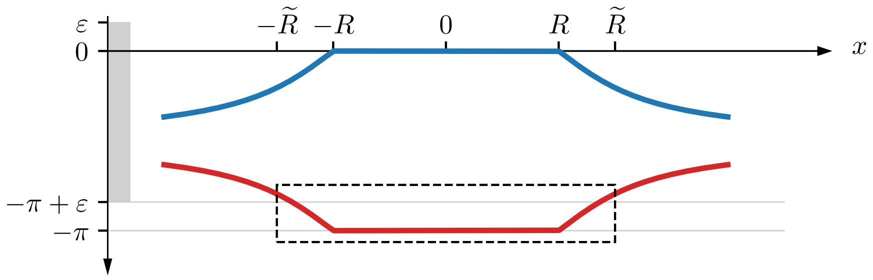

Figure 1.4: The complex arguments of terms in the special case of Example 1.4.3. ■ $\arg\left({}^{1}/_{x'_\gamma}\right)$, ■ $\arg\left(-(1+p)x'_\gamma\right)$, ■ Argument interval used in Proposition 1.4.2., --- Influence area of $(u,u)_{L^2([-\widetilde{R},\widetilde{R}])}$.

for some constant $C > 0$. The constants obscured by $\preceq$ and $\succeq$ are independent of u and v but not independent of ρ.

The stated theorem is posed in a very general form. Before we start its proof we will attempt to facilitate better insight into the key ideas. We will do so in the simplified setting of Example 1.4.3.

While it is not difficult to show the continuity of $s_\gamma(\cdot,\cdot)$, the proof of Gårdings inequality requires some creativity. We would like to apply an inverse version of the triangle inequality of the form $|a+b| \geq |a|+|b|$ and $\left|\int_A f(x)\,\mathrm{d}x\right| \geq \int_A |f(x)|\,\mathrm{d}x$. Then, the Gårding inequality would follow immediately. Although these inequalities are obviously incorrect, slightly weaker forms do hold indeed, if we pose some restrictions on the complex arguments of the terms involved. By taking the detour $|f(x)| \geq \Re[\exp(i\theta)f(x)]$ for any $\theta \in [-\pi,\pi)$, we are able to exploit the otherwise unavailable additive properties $\Re[a+b] = \Re[a]+\Re[b]$ and $\Re\left[\int_A f(x)\,\mathrm{d}x\right] = \int_A \Re[f(x)]\,\mathrm{d}x$. If we manage to apply Proposition 1.4.2 we arrive at the desired result:

$$\begin{aligned}\left|\int_A (f(x)+g(x))\,\mathrm{d}x\right| &\geq \Re\left[\exp(i\theta)\int_A (f(x)+g(x))\,\mathrm{d}x\right]\\ &= \int_A \left(\Re[\exp(i\theta)f(x)]+\Re[\exp(i\theta)g(x)]\right)\mathrm{d}x\\ &\overset{1.4.2}{\succeq} \int_A |f(x)|\,\mathrm{d}x + \int_A |g(x)|\,\mathrm{d}x.\end{aligned}$$

We will have to find bounds for the argument of the terms ${}^{1}/_{x'_\gamma}$ and $-\rho_\gamma x'_\gamma$. In the setting of Example 1.4.3, the second expression becomes $-(1+\mathbb{1}_{[-1,1]}(x))x'_\gamma$ and since p is non-negative and real, it has no influence on the argument, which is to say $\arg\left(-(1+\mathbb{1}_{[-1,1]}(x))x'_\gamma\right) = \arg(-x'_\gamma)$. Seeing further that ${}^{1}/_{x'_\gamma} = {}^{\overline{x'_\gamma}}/_{|x'_\gamma|^2}$ we get $\arg\left({}^{1}/_{x'_\gamma}\right) = \arg\left(\overline{x'_\gamma}\right) = -\arg\left(x'_\gamma\right)$ and can make sense of Figure 1.4. Outside of the interval $[-\widetilde{R},\widetilde{R}]$ it will be possible to restrict the complex argument of terms to an interval of less than π width. Inside this interval the term $(u,u)_{L^2([-\widetilde{R},\widetilde{R}])}$ is used. It allows us to shift the complex argument of the mass term $\left(C-(1+\mathbb{1}_{[-1,1]}(x))x'_\gamma\right)u\overline{v}$ into an arbitrarily small neighborhood of 0.

Proof of Theorem 1.4.10. The first claim follows quickly from the asymptotic constraint posed on ρ_γ:

$$|s_\gamma(u,v)| \leq \max(1,\|\rho_\gamma\|_{L^\infty(\mathbb{R})})(u,v)_{H^1_\gamma(\mathbb{R})} \preceq \|u\|_{H^1_\gamma(\mathbb{R})}\|v\|_{H^1_\gamma(\mathbb{R})}\,.$$

We would like to show the coercive property separately on the intervals $(-\infty, -\widetilde{R})$, $[-\widetilde{R}, -R)$, $[-R, R]$, $(R, \widetilde{R}]$ and $(\widetilde{R}, \infty)$. This requires the intermediate step

$$\left| s_\gamma(u,u) + C(u,u)_{L^2([-\widetilde{R},\widetilde{R}])} \right| \geq \Re\left[\exp(i\theta) \left(s(u,u) + C(u,u)_{L^2([-\widetilde{R},\widetilde{R}])} \right) \right],$$

with some yet to be determined $\theta \in [-\pi, \pi)$. The subsequent goal is the application of Proposition 1.4.2 in each of these intervals, which requires us to show that the argument of all components of $s_\gamma(u,u) + C(u,u)_{L^2([-\widetilde{R},\widetilde{R}])}$ are restricted to the same fixed complex half plane (with an ε to spare). The proofs for the exterior sections $(-\infty, -\widetilde{R})$ and $(\widetilde{R}, \infty)$ as well as $[-\widetilde{R}, -R)$ and $(R, \widetilde{R}]$ are entirely analogous. Therefore, we will only show one of each. As an initial step, it is helpful to form the derivative of x_γ. We have

$$x'_\gamma(x) := \begin{cases} 1, & x \in [-R, R] \\ 1 + i\alpha\tau'(|x| - R), & \text{otherwise} \end{cases}.$$

The case $x \in (R, \widetilde{R}]$: Combining terms on the left hand side we get

$$I_{(R,\widetilde{R}]} := \int_R^{\widetilde{R}} \frac{1}{x'_\gamma(x)} \left| u'(x) \right|^2 \mathrm{d}x + \int_R^{\widetilde{R}} \left(C - \rho_\gamma(x) x'_\gamma(x) \right) |u(x)|^2 \mathrm{d}x.$$

We are interested in the argument of the terms $1/x'_\gamma$ and $C - \rho_\gamma x'_\gamma$. Since $1/x'_\gamma = \overline{x'_\gamma}/|x'_\gamma|^2$, we have $\arg(1/x'_\gamma) = \arg(\overline{x'_\gamma}) = -\arg(x'_\gamma)$. In the currently chosen domain we have $\Re[x'_\gamma] = 1 > 0$ and $\tau' \geq 0$ by definition of deformation functions, which implies $\arg(x'_\gamma) \subseteq [0, \frac{\pi}{2}]$ and $\arg(1/x'_\gamma) \subseteq [-\frac{\pi}{2}, 0]$. The term $\rho_\gamma x'_\gamma$ is continuous and therefore bounded in the interval $(R, \widetilde{R}]$. Thus, the range of $C - \rho_\gamma x'_\gamma$ is subset of some ball $B_{\delta(\widetilde{R})}(C)$ with radius δ dependent on $\widetilde{R}$. For sufficiently large C we can restrict $\arg\left(C - \rho_\gamma x'_\gamma\right)$ to the interval $(-\varepsilon_1, \varepsilon_1)$ for an arbitrarily small $\varepsilon_1 > 0$. In summary, we are now able to apply Proposition 1.4.2 on the interval $(R, \widetilde{R}]$ with some θ satisfying $[\theta - (\frac{\pi}{2} - \varepsilon_1), \theta + (\frac{\pi}{2} - \varepsilon_1)] \supseteq [-\frac{\pi}{2}, \varepsilon_1]$. This leads to

$$\begin{aligned} \Re\left[\exp(i\theta) I_{(R,\widetilde{R}]} \right] &= \int_R^{\widetilde{R}} \Re\left[\exp(i\theta) 1/x'_\gamma(x) \right] \left| u'(x) \right|^2 \mathrm{d}x \\ &\quad + \int_R^{\widetilde{R}} \Re\left[\exp(i\theta) \left(C - \rho_\gamma(x) x'_\gamma(x) \right) \right] |u(x)|^2 \mathrm{d}x \\ &\succeq \int_R^{\widetilde{R}} \left| 1/x'_\gamma(x) \right| \left| u'(x) \right|^2 \mathrm{d}x + \int_R^{\widetilde{R}} \left| C - \rho_\gamma(x) x'_\gamma(x) \right| |u(x)|^2 \mathrm{d}x \\ &\geq \min\Big(1, \min_{[-\widetilde{R},\widetilde{R}]} \left| C/x'_\gamma - \rho_\gamma \right| \Big) \|u\|^2_{H^1_\gamma((R,\widetilde{R}])}. \end{aligned}$$

The constant $\min_{[-\widetilde{R},\widetilde{R}]} \left| C/x'_\gamma - \rho_\gamma \right|$ in the last line is well defined, and the previously chosen C already guarantees that it is positive.

The case $x \in [-R, R]$: In this case we have simply $x'_\gamma = 1$ and $\arg(1/x'_\gamma) = 0$. Choosing C sufficiently large, the argument of $C - \rho_\gamma x'_\gamma = C - \rho_\gamma$ can again be restricted to the interval $(-\varepsilon_1, \varepsilon_1)$ by using the same argument as in the case of $x \in (R, \widetilde{R}]$.

The case $x \in (\widetilde{R}, \infty)$: We use the same approach as in the previous intervals on the slightly different terms $1/x'_\gamma$ and $-\rho_\gamma x'_\gamma$. As before, we have $\arg(1/x'_\gamma) \subseteq [-\frac{\pi}{2}, 0]$. The requirements on the argument of $\rho_\gamma x'_\gamma$ guarantee the existence of a $\theta \in (-\frac{\pi}{2}, 0)$ and $\varepsilon_2 > 0$ such that $\arg(1/x'_\gamma) \cup \arg(\rho_\gamma x'_\gamma) \subseteq [\theta - (\frac{\pi}{2} - \varepsilon_2), \theta + (\frac{\pi}{2} - \varepsilon_2)]$. Using the notation

$$I_{(\widetilde{R},\infty)} := \int_{\widetilde{R}}^\infty \frac{1}{x'_\gamma(x)} \left| u'(x) \right|^2 \mathrm{d}x + \int_R^{\widetilde{R}} \rho_\gamma(x) x'_\gamma(x) |u(x)|^2 \mathrm{d}x.$$

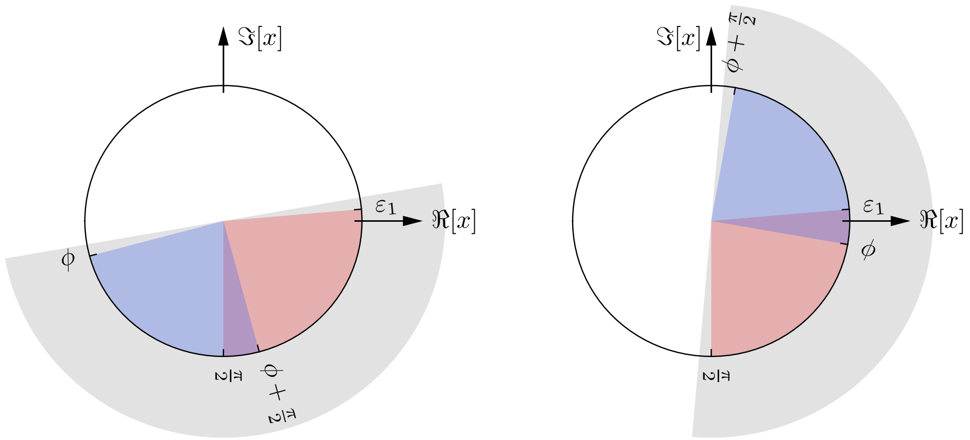

Figure 1.5: A possible argument distribution for the cases ϕ close to 0 *(left)* and ϕ close to π *(right)*. ■ The argument interval containing $\arg(-\rho_\gamma(x)x'_\gamma(x))$ in the case $x \in (\widetilde{R}, \infty)$. ■ The argument interval containing the argument of all other terms involved. ■ The complex halfspace used in Proposition 1.4.2.

we get

$$\begin{aligned}\Re\left[\exp(i\theta)I_{(\widetilde{R},\infty)}\right] &= \int_{\widetilde{R}}^{\infty} \Re\left[\exp(i\theta)^1/x'_\gamma(x)\right]\left|u'(x)\right|^2 \mathrm{d}x \\ &\quad + \int_R^{\widetilde{R}} \Re\left[\exp(i\theta)\rho_\gamma(x)x'_\gamma(x)\right]\left|u(x)\right|^2 \mathrm{d}x \\ &\succeq \int_{\widetilde{R}}^{\infty} \left|^1/x'_\gamma(x)\right|\left|u'(x)\right|^2 \mathrm{d}x + \int_{\widetilde{R}}^{\infty} \left|\rho_\gamma(x)x'_\gamma(x)\right|\left|u(x)\right|^2 \mathrm{d}x \\ &\geq \min\left(1, \tfrac{|\rho_0|}{2}\right)\|u\|^2_{H^1_\gamma((\widetilde{R},\infty))}.\end{aligned}$$

The parameters θ, ε_1 and ε_2 can be chosen such that the interval $[\theta - \frac{\pi}{2} + \varepsilon_2, \theta + \frac{\pi}{2} - \varepsilon_2]$ contains the arguments of all terms and all cases (see Figure 1.5). □

Let $E_{\widetilde{R}}$ be the embedding $E_{\widetilde{R}}\colon H^1_\gamma([-\widetilde{R}, \widetilde{R}]) \to L^2([-\widetilde{R}, \widetilde{R}])$. It is compact according to Remark 1.4.9 and can be easily extended to an embedding $E\colon H^1_\gamma(\mathbb{R}) \to L^2([-\widetilde{R}, \widetilde{R}])$ with the assignment $Ev := E_{\widetilde{R}}(v|_{[-\widetilde{R},\widetilde{R}]})$. The restriction operator is continuous because $\|v|_{[-\widetilde{R},\widetilde{R}]}\|_{H^1_\gamma([-\widetilde{R},\widetilde{R}])} \leq \|v\|_{H^1_\gamma(\mathbb{R})}, \forall v \in H^1_\gamma(\mathbb{R})$ which makes the extension E compact as well, since it is the composition of the continuous restriction operator $\cdot|_{[-\widetilde{R},\widetilde{R}]} : H^1_\gamma(\mathbb{R}) \to H^1_\gamma([-\widetilde{R}, \widetilde{R}])$ and the compact embedding $E_{\widetilde{R}}$. Using the embedding E, we can write the Gårding inequality (1.4.4) as

$$\left|s_\gamma(u,u) + (Ku,u)_{H^1_\gamma(\mathbb{R})}\right| \succeq \|u\|^2_{H^1_\gamma(\mathbb{R})}, \quad u, \in H^1_\gamma(\mathbb{R}),$$

with the compact operator $K = CE^*E$. For equations of Helmholtz-type the constant C – and therefore also the operator K – will depend on ω, i.e. $K = K(\omega)$.

1.5 Results for equations of Helmholtz-type

The complex scaled variational formulation of Helmholtz-type equations is obtained from the scaled sesquilinear form s_γ with the substitution $\rho(x) = \omega^2(1 + p(x))$. In chapter 2 we will use a similar substitution of ρ to arrive at the time-independent

Schrödinger equation.

For now we get:

$$\text{Find } u \in H^1_\gamma(\mathbb{R})\colon s^H_\gamma(u,v) = f(v), \quad v \in H^1_\gamma(\mathbb{R}), \tag{1.5.1}$$

where

$$\begin{aligned} s^H_\gamma(u,v) &:= \int_{\mathbb{R}} \left(\frac{1}{x'_\gamma} u'\overline{v}' - \omega^2(1+p)x'_\gamma u\overline{v} \right) \mathrm{d}x, \\ f(v) &:= \int_{\mathbb{R}} gv \, \mathrm{d}x. \end{aligned}$$

The proof of Theorem 1.4.10 alone is not useful to us yet, since it is not immediately obvious how it applies to Helmholtz-type equations. In order to quickly remedy any confusion, we prove the following corollary.

Corollary 1.5.1. *(to Theorem 1.4.10) Let* $\omega \in \mathbb{C}$*,* $\Re[\omega] > 0$ *and* $p \in L^\infty(\mathbb{R})$ *with bounded support* $\operatorname{supp} p \subset (-R, R)$*. If* τ *is a deformation function satisfying*

$$\liminf_{x\to\infty} \arg(x'_\gamma(x)) > -2\arg(\omega), \tag{1.5.2}$$

then Theorem 1.4.10 is applicable to complex scaled Helmholtz-type variational formulations, i.e. $\rho(x) = \omega^2(1+p(x))$*.*

Proof. We have to show that $\rho(x) = \omega^2(1+p(x))$ satisfies all conditions posed in the premise of Theorem 1.4.10. Most are easily confirmed, as $\omega^2(1+p(x))$ is bounded in Ω_{int} and constant otherwise which immediately implies the holomorphic property in $\{ x \in \mathbb{C} : \Re[x] \in \Omega_{\text{ext}} \} \supset \operatorname{crit} x_\gamma$. What is left is the abstract requirement

$$\exists \phi \in (0,\pi)\colon \ \arg(\rho_\gamma(x)x'_\gamma(x)) \in [\phi, \phi + \pi/2] \,,$$

which translates to

$$\exists \phi \in (0,\pi)\colon \ \arg(\omega^2(1 + i\alpha\tau'(|x|-R))) \in [\phi, \phi + \pi/2] \,.$$

Since $\tau'(x) > 0$, there holds $\arg(1 + i\alpha\tau'(|x|-R)) \in [0, \frac{\pi}{2}]$ and due to $\Re[\omega] > 0$ we know $\arg(\omega^2) < \pi$. Consequently, we can bound the argument within an interval of width $\frac{\pi}{2}$ and the required parameter ϕ will never exceed π. On the other hand we need the existence of some $\varepsilon > 0$ such that $\arg(\omega^2(1 + i\alpha\tau'(|x|-R))) \geq \varepsilon > 0$ for large x, or equivalently $\liminf_{x\to\infty} \arg(1 + i\alpha\tau'(|x|-R)) > -2\arg(\omega)$, which is the condition posed in the beginning. Again, the argument holds for $x < R$ as well. □

Remark 1.5.2. *For* $x > R$ *we have* $x'_\gamma(x) = 1 + i\alpha\tau'(x-R)$*. Since* $\liminf_{x\to\infty} \tau'(x) > 0$ *by definition of deformation functions, there holds*

$$\liminf_{x\to\infty} \arg(x'_\gamma(x)) > 0,$$

and condition (1.5.2) always holds if ω *is real and positive or* $\arg(\omega) > 0$*.*

What is left to show is how solutions of the unscaled problem (1.2.8) are related to solutions of the scaled problem (1.5.1). This will only be possible for certain deformation functions τ and scaling constants α.

We call a function $f\colon \mathbb{R} \to \mathbb{R}$ polynomially bounded if there exists $k \in \mathbb{N}$ and $C > 0$ such that $f(x) \leq x^k$ for all $x \geq C$.

Proposition 1.5.3. *Let $\omega \in \mathbb{C}$ with $\Re[\omega] > 0$ and u be a solution satisfying representation (1.2.11). Given a deformation function τ and scaling parameter α, assume that τ' is polynomially bounded and there holds either*

(i) $\tau(x) = x$ *and* $\alpha > -\frac{\Im[w]}{\Re[w]}$*, or*

(ii) τ *is increasing at superlinear pace, i.e.* $\lim_{x\to\infty} \frac{x}{\tau(x)} = 0$ *and* $\alpha > 0$*,*

then $u \circ u_\gamma =: u_\gamma \in H^1_\gamma(\mathbb{R})$ *and* $|u_\gamma|$ *decays exponentially in* Ω_{ext}*.*

Proof. In order to determine the space membership $u_\gamma \in H^1_\gamma(\mathbb{R})$ and its asymptotic behavior it is sufficient to analyze u_γ in Ω_{ext}. We use solution representation (1.2.11) for $x \in \Omega^+_{\text{ext}}$ and get

$$u_\gamma(x) = u_{\text{int}}(R) \exp(i\omega(x_\gamma - R)).$$

We need to show that

$$\|u_\gamma\|_{H^1_\gamma(\Omega^+_{\text{ext}})} = \int_{\Omega^+_{\text{ext}}} \left(|1/x'_\gamma||u'_\gamma|^2 + |x'_\gamma||u_\gamma|^2\right) \mathrm{d}x < \infty. \tag{1.5.3}$$

In the chosen interval we have $x_\gamma = x + i\alpha\tau(x - R)$ and $x'_\gamma = 1 + i\alpha\tau'(x - R)$, which shows that both $|x'_\gamma|$ and $|1/x'_\gamma|$ are polynomially bounded. Furthermore, using the simplifying expression $u_0 \coloneqq u_{\text{int}}(R)\exp(-i\omega R)$ there holds

$$\begin{aligned} u_\gamma &= u_0 \exp(i\omega x_\gamma) \quad \text{and} \\ u'_\gamma &= u_0 i\omega x'_\gamma \exp(i\omega x_\gamma). \end{aligned}$$

With the chosen upper bound on τ' all terms of (1.5.3) except $u_\gamma = u_0 \exp(i\omega x_\gamma)$ are polynomially bounded. Therefore, we have $u_\gamma \in H^1_\gamma(\mathbb{R})$ if and only if $|u_\gamma|$ decays exponentially. We can estimate

$$\begin{aligned} |u_\gamma(x)| &= |u_{\text{int}}(R)\exp(-i\omega R)||\exp(i\omega x_\gamma)| \\ &= |u_0| \exp\Big(\Re\Big[i\omega\left(x + i\alpha\tau(x - R)\right)\Big]\Big) \\ &= |u_0| \exp(-\Im[\omega]x - \alpha\Re[\omega]\tau(x - R)). \end{aligned}$$

We see, that exponential decay of $|u_\gamma|$ is equivalent to $-\Im[\omega]x - \alpha\Re[\omega]\tau(x - R) < 0$ for large x. In the easiest case of $\tau(x) = x$, this condition translates to

$$\begin{aligned} & -\Im[\omega]x - \alpha\Re[\omega](x - R) < 0 \\ \Leftrightarrow \qquad & -\frac{\Im[\omega]}{\Re[\omega]} < \alpha\Big(1 - \frac{R}{x}\Big), \end{aligned}$$

resulting in the claimed bound for α. Otherwise we get

$$\begin{aligned} & -\Im[\omega]x - \alpha\Re[\omega]\tau(x - R) < 0 \\ \Leftrightarrow \qquad & -\frac{\Im[\omega]}{\alpha\Re[\omega]}\frac{x}{\tau(x - R)} < 1, \end{aligned}$$

which holds for any superlinear τ and sufficiently large x. The same argument can be repeated for $x \in \Omega^-_{\text{ext}}$. □

The bounding condition on τ' used in Proposition 1.5.3 is not necessarily an exhaustive description of all triplets (u, τ, α) for which $u_\gamma \in H^1_\gamma(\mathbb{R})$ and $|u_\gamma|$ decays exponentially. However, this behavior will be necessary in the following theorem. It will give us another characterization of the *radiating* property and states that for certain ω and scaling profiles (τ, α) the capability of u_γ to act as a solution of (1.5.1) is equivalent to u being a radiating solution of (1.2.8).

Theorem 1.5.4. *Let $\omega \in \mathbb{C}$ where $\Re[\omega] > 0$, $p \in L^\infty(\mathbb{R})$ and $g \in L^2(\mathbb{R})$ with bounded supports $\operatorname{supp} p, \operatorname{supp} g \subseteq \Omega_{int}$. Further, let u be a solution satisfying representation (1.2.11) and (τ, α) a deformation function and scaling parameter such that $u_\gamma = u \circ x_\gamma \in H^1_\gamma(\mathbb{R})$ and $|u_\gamma|$ decays exponentially in Ω_{ext}. Then the following two statements are equivalent:*

(i) $u \in H^1_{\mathrm{loc}}(\mathbb{R})$ is a radiating solution of (1.2.8).

(ii) $u_\gamma = u \circ x_\gamma \in H^1_\gamma(\mathbb{R})$ solves the scaled variational problem (1.5.1).

Proof. Assume *(i)*: Solutions of (1.2.8) are smooth in the exterior domain and satisfy (1.2.4). Consequently u_γ satisfies

$$-\left(\frac{u_\gamma'}{x_\gamma'}\right)' - \omega^2 x_\gamma' u_\gamma = 0, \quad x \in \Omega^+_{\mathrm{ext}}. \tag{1.5.4}$$

According to Proposition 1.5.3 the scaled solution u_γ lies in $H^1_\gamma(\mathbb{R})$ which allows us to multiply with test functions $w \in H^1_\gamma(\mathbb{R})$ and use partial integration as usual, to get

$$\begin{aligned}\int_{\Omega^+_{\mathrm{ext}}} \left(\frac{1}{x_\gamma'} u_\gamma' \overline{w'} - \omega^2 x_\gamma' u_\gamma \overline{w}\right) \mathrm{d}x &= -\left(\frac{u_\gamma'}{x_\gamma'}\right)(R)\overline{w(R)} \\ &= -u'(R)\overline{w(R)} \\ &= -\operatorname{DtN}_+[u(R)]\overline{w(R)}.\end{aligned}$$

After performing analogous steps in Ω^-_{ext} and using (1.2.7) we get

$$\int_{\Omega_{\mathrm{ext}}} \left(u'\overline{v'} - \omega^2 u\overline{v}\right) \mathrm{d}x = \int_{\Omega_{\mathrm{ext}}} \left(\frac{1}{x_\gamma'} u_\gamma' \overline{w'} - \omega^2 x_\gamma' u_\gamma \overline{w}\right) \mathrm{d}x,$$

for all $(v, w) \in H^1_{\mathrm{comp}}(\mathbb{R}) \times H^1_\gamma(\mathbb{R})$ satisfying $v(R) = w(R)$ which in conjunction with $u = u_\gamma$ on the interior domain implies *(ii)*.

Assume *(ii)*: The test space $H^1_\gamma(\mathbb{R})$ contains test functions w that satisfy $\operatorname{supp} w \subset \Omega^+_{\mathrm{ext}}$ and $w(R) = 0$. For such w there holds

$$\int_{\Omega^+_{\mathrm{ext}}} \left(\frac{1}{x_\gamma'} u_\gamma' \overline{w'} - \omega^2 x_\gamma' u_\gamma \overline{w}\right) \mathrm{d}x = 0.$$

Regularity results for elliptic differential equations guarantee that $u_{\gamma,+} := u_\gamma|_{\Omega^+_{\mathrm{ext}}} \in H^2((R, \infty))$. Using partial integration, we see that $u_{\gamma,+}$ satisfies (1.5.4) and therefore can be written as

$$u_{\gamma,+}(x) = C_1 \exp\left(i\omega(x_\gamma - R)\right) + C_2 \exp\left(-i\omega(x_\gamma - R)\right), \quad x \in \Omega^+_{\mathrm{ext}},$$

for some $C_1, C_2 \in \mathbb{C}$. Since the chosen deformation parameters τ and α guarantee the exponential decay of $u_{\gamma,+}(x)$ and $u_\gamma(x) \in H^1_\gamma(\mathbb{R})$, it is implied that $C_2 = 0$ and we get

$u_{\gamma,+}(R) = i\omega x'_\gamma(R) u'_{\gamma,+}(R)$. We return to general test functions $w \in H^1_\gamma(\mathbb{R})$ and apply partial integration

$$\begin{aligned}\int_{\Omega^+_{\text{ext}}} \left(\frac{1}{x'_\gamma} u'_\gamma \overline{w'} - \omega^2 x'_\gamma u_\gamma \overline{w} \right) \mathrm{d}x &= -i\omega u_\gamma(R) \overline{w(R)} \\ &= -\operatorname{DtN}_+[u(R)]\overline{w(R)}.\end{aligned}$$

Once again, we repeat the argument in Ω^-_{ext} and argue that $x_\gamma = x$ in the interior domain. □

Chapter 2

The time-independent Schrödinger equation

2.1 Preamble

The non-relativistic time-dependent Schrödinger equation

$$i\hbar\frac{\partial}{\partial t}\Psi(x,t) = -\frac{\hbar^2}{2m}\frac{\partial^2}{\partial x^2}\Psi(x,t) + V(x)\Psi(x,t) \tag{2.1.1}$$

describes the movement of a single particle of mass m and impulse p in an electric field. Its total energy E is the sum of its kinetic energy $\frac{p^2}{2m}$ and potential energy $V(x)$. Here $\hbar$ denotes the reduced Planck constant.

To isolate the time dependence of (2.1.1), a method of separation of variables is used. By taking the ansatz

$$\Psi(x,t) = \psi(x)\exp\Bigl(-\tfrac{iEt}{\hbar}\Bigr),$$

and substituting it into (2.1.1) we get

$$E\psi(x)\exp\Bigl(-\tfrac{iEt}{\hbar}\Bigr) = -\frac{\hbar^2}{2m}\frac{\mathrm{d}^2\psi(x)}{\mathrm{d}x^2}\exp\Bigl(-\tfrac{iEt}{\hbar}\Bigr) + V(x)\psi(x)\exp\Bigl(-\tfrac{iEt}{\hbar}\Bigr).$$

We cancel the term $\exp\Bigl(-\tfrac{iEt}{\hbar}\Bigr)$ on both sides and arrive at the time-independent Schrödinger equation

$$-\frac{\hbar^2}{2m}\frac{\mathrm{d}^2}{\mathrm{d}x^2}\psi(x) + V(x)\psi(x) = E\psi(x). \tag{2.1.2}$$

Let I be the identity operator on $H^2_{\mathrm{loc}}(\Omega)$, then (2.1.2) is an eigenvalue equation of the Hamilton operator

$$H = \Bigl(-\frac{\hbar^2}{2m}\frac{\mathrm{d}^2}{\mathrm{d}x^2} + V\Bigr)I. \tag{2.1.3}$$

Renaming and rescaling of terms leads to the *mathematicians* time-independent Schrödinger equation with an additional abstract radiation condition

$$-u'' + V(x)u = \lambda^2 u, \quad x \in \Omega, \tag{2.1.4}$$

$$u \text{ is radiating for } |x| \to \infty. \tag{2.1.5}$$

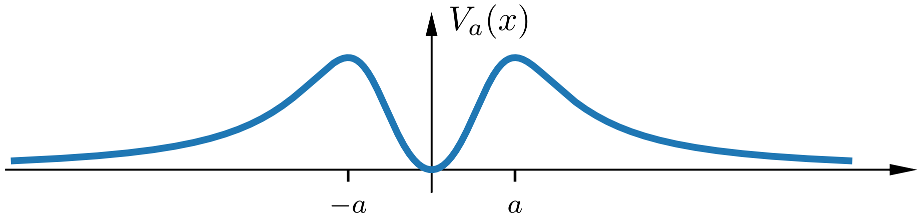

Figure 2.1: The shape of the studied potentials $V_a(x) = x^2(1 + (x/a)^4)^{-1}$.

The meaning of condition (2.1.5) is not clear yet since our previous definition of radiating solutions is invalid for solutions $u \in H^2_{\text{loc}}$ of (2.1.4).

We will exclusively work with the equation in its variational formulation:

$$\text{find } u \in H^1_{\text{loc}} : s_\lambda(u, v) = 0, \quad v \in H^1_{\text{comp}}, \qquad (2.1.6)$$
$$u \text{ is radiating for } |x| \to \infty,$$

where the sesquilinear form $s_\lambda(\cdot, \cdot)$ on $H^1(\mathbb{R}) \times H^1(\mathbb{R})$ is obtained by multiplying with test functions $v \in H^1(\mathbb{R})$ and partial integration as usual:

$$s_\lambda(u, v) := \int_{\mathbb{R}} \left(u'\overline{v'} - (\lambda^2 - V(x))u\overline{v} \right) \mathrm{d}x. \qquad (2.1.7)$$

Definition 2.1.1. *(Resonance of the Hamilton operator) Let $\Omega = \mathbb{R}$, $u \in H^1_{loc} \setminus \{0\}$ and $\Re[\lambda] > 0$. If (u, λ) solves the variational formulation (2.1.6), then λ is said to be a resonance of the Hamilton operator (2.1.3).*

2.2 Decaying potentials

We are mainly interested in rational potential functions of the form

$$V_a(x) = \frac{x^2}{1 + \left(\frac{x}{a}\right)^4}, \qquad (2.2.1)$$

where $a > 0$. For small x, these potentials are approximations to the harmonic oscillator with potential function $V(x) = x^2$, and decay at quadratic pace for $|x| \to \infty$. The origin point is a local minimum and called a potential well. In classical physics, potential wells can act as a trap for particles that possess an insufficient amount of energy – a fundamental property, that changes in the realm of quantum physics. Due to its probabilistic nature, a quantum particle may *tunnel* through the walls of a potential well.

The eigenpairs (λ_n, ψ_n) of the Hamilton operator represent stable energy states and the probability densities of quantum wave functions. We expect lower energy states to be close to real values, as the quantum wave function is mostly trapped in the potential well. As higher energy states are approached, more energy surpasses the well and is transported outward. This is reflected in the imaginary component of λ_n.

2.2.1 Radiating solutions

In the previous chapter we have treated Helmholtz-type equations $-u''(x) - \omega^2(1 + p(x))u(x) = g(x)$, and required the function p to be zero in the exterior domain. In this sense, the exterior domain was *homogeneous*. Since $\operatorname{supp} V_a(x) = \mathbb{R}$, we call the exterior domain of this chapter *inhomogeneous*. The formulation of a radiation condition for the time-independent Schrödinger equation is more difficult since its solutions are not explicitly known in the exterior domain. We will pose it in the form of a constraint on the asymptotic decay of solutions.

Definition 2.2.1. *(Radiation condition (2.1.5)) A solution u of (2.1.4) is said to be radiating if and only if there exist constants $C_1 > 0$ and $C_2 \in \mathbb{C}$ with $\Re[C_2] > 0$, such that*

$$|u(x)| \leq |\exp(iC_2 x)|,$$

for all $x \in \{ x \in \mathbb{C} : \Re[iC_2 x] < -C_1 \}$.

Note, that for solutions u_{ext} of (1.2.4) this radiation condition coincides with the condition posed in Definition 1.2.1.

2.2.2 Results for inhomogeneous exterior domains

The application of Theorem 1.4.10 to the time-independent Schrödinger equation is done in a manner similar to the previous chapter. The following corollary serves as an analog to Corollary 1.5.1.

For two sets $A, B \subseteq \mathbb{R}$ and a scalar $c \in \mathbb{R}$ we will use the notation $A + B$ to express the set $\{ a + b : a \in A, b \in B \}$ and $c + A$ for the set $\{ c + a : a \in A \}$.

Corollary 2.2.2. *(to Theorem 1.4.10) Let $\lambda \in \mathbb{C}$ with $\Re[\lambda] > 0$ and V_a a potential of the form (2.2.1) for some $a > 0$. If τ is a deformation function and α a scaling parameter such that*

$$\frac{a}{\sqrt{2}}(\pm 1 \pm i) \notin \operatorname{crit} x_\gamma,$$

and there holds

$$\liminf_{x\to\infty} \arg(x'_\gamma(x)) > -2\arg(\lambda),$$

then Theorem 1.4.10 is applicable to the weak form of the Schrödinger equation (2.1.6) with potential V_a and $\rho(x) = \lambda^2 - V_a(x)$.

Proof. The denominator of V_a is a polynomial of degree four. It has exactly four zeros, which are the poles of V_a. Elementary operations show that these poles lie at $\frac{a}{\sqrt{2}}(\pm 1 \pm i)$. Therefore, V_a is holomorphic in $\operatorname{crit} x_\gamma$ if and only if $\frac{a}{\sqrt{2}}(\pm 1 \pm i) \notin \operatorname{crit} x_\gamma$.

The potential is bounded in Ω_{int} and since $\lim_{|x|\to\infty} V_a(x) = 0$, we have

$$\lim_{|x|\to\infty} \rho_\gamma(x) = \lim_{|x|\to\infty} (\lambda^2 - V_a(x_\gamma)) = \lambda^2 =: \rho_0.$$

The requirement $\Re[\lambda] > 0$ implies $\arg \lambda^2 \notin \mathbb{C} \setminus \mathbb{R}_{\leq 0}$. Since the complex argument operator is continuous on $\mathbb{C} \setminus \mathbb{R}_{\leq 0}$, there holds

$$\lim_{|x|\to\infty} \arg(\rho_\gamma(x)) = \lim_{|x|\to\infty} \arg(\lambda^2 - V_a(x_\gamma)) = \arg(\lambda^2).$$

By the definition of deformation functions, we know $\liminf_{x\to\infty} \tau'(x) > 0$, which implies the existence of some $\beta > 0$ and $c_1 > 0$ such that $\arg(x'_\gamma) = \arg(1+i\alpha\tau'(|x|-R)) \in [\beta, \frac{\pi}{2}]$ for $|x| > c_1$. We combine these facts and, after assuring ourselves that arg acts continuously on all terms, there exists an arbitrarily small $\varepsilon > 0$ and $c_2(\varepsilon) > 0$ such that

$$\arg(\rho_\gamma(x)x'_\gamma) = \arg(\rho_\gamma(x)) + \arg(x'_\gamma) \in \left(\left[\arg(\lambda^2) - \varepsilon, \arg(\lambda^2) + \varepsilon\right] + \left[\beta, \frac{\pi}{2}\right]\right) =: I,$$

for all $|x| > c_2(\varepsilon)$. We can rewrite $I = \arg(\lambda^2) + [\beta - \varepsilon, \frac{\pi}{2} + \varepsilon]$ and see, that for $\varepsilon < \frac{\beta}{2}$ the complex argument lies within an interval of less than $\frac{\pi}{2}$ width. It remains to be shown, that there exists ϕ within bounds $(0, \pi)$ such that $I \subseteq [\phi, \phi + \frac{\pi}{2}]$. For the upper bound of ϕ, we set $\phi = \arg(\lambda^2) + \varepsilon$ to get $\phi < \pi$ for sufficiently small ε and $I = \phi + [\beta - 2\varepsilon, \frac{\pi}{2}]$. The lower bound is critical if $\arg(\lambda^2) < 0$ and follows from the initial requirement $\liminf_{x\to\infty} \arg(x'_\gamma(x)) > -\arg(\lambda^2)$. It allows us to choose β more strictly as $\beta > -\arg(\lambda^2) + 2\varepsilon > 0$ and for $\phi = \varepsilon > 0$ this results in

$$\begin{aligned} I &= \arg(\lambda^2) + \left[\beta - \varepsilon, \frac{\pi}{2} + \varepsilon\right] \\ &= \varepsilon + \left[\arg(\lambda^2) + \beta - 2\varepsilon, \arg(\lambda^2) + \frac{\pi}{2}\right] \\ &\subseteq \phi + \left[0, \arg(\lambda^2) + \frac{\pi}{2}\right]. \end{aligned}$$

□

2.2.3 Necessary conditions for the equivalence of scaled and unscaled solutions

In Theorem 1.5.4 of the last chapter conditions were proven under which functions u, that solve the complex scaled variational problem (1.5.1), are exactly the complex scaled radiating solutions of the unscaled formulation. We will show necessary conditions for a similar result in the framework of the time-independent Schrödinger equation and potentials V_a. Numerical tests suggest that these conditions might even be sufficient.

The complex scaled variational formulation for the time-independent Schrödinger equation reads:

$$\text{Find } u \in H^1_\gamma(\mathbb{R})\colon s^S_\gamma(u, v) = 0, \quad v \in H^1_\gamma(\mathbb{R}), \tag{2.2.2}$$

where

$$s^S_\gamma(u, v) := \int_{\mathbb{R}} \left(\frac{1}{x'_\gamma} u'\overline{v'} - (\lambda^2 - V_a(x_\gamma))x'_\gamma u\overline{v}\right) \mathrm{d}x,$$

is a sesquilinear form on $H^1_\gamma(\mathbb{R}) \times H^1_\gamma(\mathbb{R})$.

Lemma 2.2.3. *Let $g \in L^\infty(\mathbb{R})$ and u be a solution to the variational problem: Find $u \in H^1_{\mathrm{loc}}(\mathbb{R})$ such that $s(u, v) = 0$ for all $v \in H^1_{\mathrm{comp}}(\mathbb{R})$, where*

$$s(u, v) = \int_{\mathbb{R}} \left(u'v' - guv\right) \mathrm{d}x,$$

and u satisfies the asymptotic constraint

$$|u(x)| + \left|u'(x)\right| \leq C_2 |\exp(C_1 x)|, \quad x \in \{ y \in \mathbb{C} : \Re[y] > -1 \},$$

for some $C_3 > C_1 \geq 1$ and $C_2 > 0$. Then $s(u, w) = 0$, where $w\colon \mathbb{C} \to \mathbb{C}$ is a test function in $\in H^1(\mathbb{R}) \setminus H^1_{\text{comp}}(\mathbb{R})$ and is defined by

$$w(x) := \begin{cases} \exp(-C_3 x), & 0 \leq \Re[x] \\ \exp(-C_3 x)(1 + \Re[x]), & -1 \leq \Re[x] < 0 \\ 0, & \Re[x] < -1 \end{cases}.$$

Proof. Our goal is to apply the dominated convergence theorem. It is easy to see, that $w|_{\mathbb{R}} =: w_{\mathbb{R}} \in H^1(\mathbb{R})$ and $|w'_{\mathbb{R}}| \leq (1 + C_3) w_{\mathbb{R}}$. In the following we will only work with w on the real axis and omit the subscript of $w_{\mathbb{R}}$ and use the asymptotic constraint on u to estimate

$$\begin{aligned} |s(u, w)| &= \left| \int_{\mathbb{R}} \Big(u'w' - guw \Big) \, \mathrm{d}x \right| \\ &\leq \int_{-1}^{\infty} (|u'w'| + |guw|) \, \mathrm{d}x \\ &\preceq \int_{-1}^{\infty} (1 + C_3)|w| \, (|u'| + |u|) \, \mathrm{d}x \\ &\preceq \int_{-1}^{\infty} (1 + C_3) \exp\big((C_1 - C_3)x\big) \, \mathrm{d}x < \infty \end{aligned}$$

We further define $w_k \in H^1_{\text{comp}}(\mathbb{R})$ as

$$w_k(x) := \begin{cases} w(x), & x \leq k \\ w(x)(k + 1 - x), & k < x \leq k + 1 \\ 0, & k + 1 < x \end{cases}.$$

Let $I(u, v) := u'v' - guv$, then $s(u, v) = \int_{\mathbb{R}} I(u, v) \, \mathrm{d}x$ and $I(u, w) - I(u, w_k)$ converges to 0 almost everywhere. Simple estimates show that $|w_k(x)| \leq |w(x)|$ and $|w'_k(x)| \leq 2|w'(x)|$, which imply $|I(u, w_k)(x)| \leq 2(|u'w'| + |guw|)$ almost everywhere. Since $(|u'w'| + |guw|)$ is integrable as seen in the estimation of $s(u, w) < \infty$ above, we can apply the dominated convergence theorem to get

$$s(u, w) = \lim_{k \to \infty} s(u, w_k) = 0.$$

□

In the next theorem the residue theorem will be required.

Definition 2.2.4. *(Residue) Let f be a holomorphic function with an isolated singularity at z_0 and define the family $\gamma_\varepsilon(t) := z_0 + \varepsilon \exp(2\pi i t)$ of closed paths around z_0. Then the value*

$$\operatorname{Res}_{z_0} f := \frac{1}{2\pi i} \int_{\gamma_\varepsilon} f(z) \, \mathrm{d}z,$$

is well defined for sufficiently small ε and called the residue of f at z_0.

Theorem 2.2.5. *(Residue theorem) Let G be an open, simply connected subset of $\mathbb{C}$ and f holomorphic on G with the exception of a set $S \subset G$ of isolated singularities. Further, let γ be a path in G which does not intersect with any points in S and denote the winding number of γ around a point a by $\nu_\gamma(a)$. Then γ revolves only around a finite number of points in S and there holds the residue formula*

$$\frac{1}{2\pi i} \int_\gamma f(z) \, \mathrm{d}z = \sum_{a \in S} \nu_\gamma(a) \operatorname{Res}_a f.$$

Proof. See [Jän11]. □

Theorem 2.2.6. *Let $a > 0$, $\lambda \in C$ with $\Re[\lambda] > 0$ and $\tau(x) = x$ the linear deformation function with scaling constant $\alpha = 1$. Further, let u be a solution to (2.1.6) that is holomorphic on an open superset O of $\overline{\operatorname{crit} x_\gamma}$ and non-zero at the poles of V_a. Assume there exist constants $C_1, C_2 > 0$ such that u satisfies the constraint*

$$|u(x)| + \left|u'(x)\right| \leq C_2 \exp(C_1 |\Re[x]|), \quad x \in \mathbb{C}. \tag{2.2.3}$$

If the following two statements are equivalent:

(i) $u \in H^1_{\text{loc}}(\mathbb{R})$ is a solution of (2.1.6),

(ii) $u_\gamma = u \circ x_\gamma \in H^1_\gamma(\mathbb{R})$ solves the scaled variational problem (2.2.2),

then V_a is holomorphic on $\operatorname{crit} x_\gamma$, or equivalently

$$\frac{a}{\sqrt{2}} (\pm 1 \pm i) \notin \operatorname{crit} x_\gamma. \tag{2.2.4}$$

Proof. There holds $\operatorname{crit}_+ x_\gamma \subseteq \{ z \in \mathbb{C} : \Re[z] \geq 0 \wedge \Im[z] \geq 0 \}$ and $\operatorname{crit}_- x_\gamma = -\operatorname{crit}_+ x_\gamma$, where for any set $A \subseteq \mathbb{C}$ the expression $-A$ denotes the set $\{ z \in \mathbb{C} : -z \in A \}$. This implies that of the four poles $\frac{a}{\sqrt{2}} (\pm 1 \pm i)$ there holds at most $\frac{a}{\sqrt{2}} (1 + i) \in \operatorname{crit}_+ x_\gamma$ and equivalently $\frac{a}{\sqrt{2}} (-1 - i) \in \operatorname{crit}_- x_\gamma$. Therefore, condition (2.2.4) reduces to $p := \frac{a}{\sqrt{2}} (1 + i) \notin \operatorname{crit}_+ x_\gamma$.

For either a set $\Gamma \subseteq \mathbb{R}$ or a path $\Gamma \colon [0, 1] \to \mathbb{C}$ we define the sesquilinear form

$$t_\Gamma(u, v) := \int_\Gamma \left(u' \overline{v'} - (\lambda^2 - V_a(x)) u \overline{v} \right) \mathrm{d}x. \tag{2.2.5}$$

Using this notation, the weak formulation (2.1.6) becomes: Find $u \in H^1_{\text{loc}}(\mathbb{R})$ such that $t_\mathbb{R}(u, v) = 0$ for all $v \colon \mathbb{C} \to \mathbb{C}$ satisfying $v|_\mathbb{R} \in H^1_{\text{comp}}(\mathbb{R})$. Similarly, the complex scaled formulation (2.2.2) can be written as: Find $u \in H^1_\gamma(\mathbb{R})$ such that $t_{x_\gamma(\mathbb{R})}(u, v) = 0$ for all v with $v_\gamma := v \circ x_\gamma$ satisfying $v_\gamma|_\mathbb{R} \in H^1_\gamma(\mathbb{R})$:

$$\begin{aligned}
t_{x_\gamma(\mathbb{R})}(u, v) &= \int_{x_\gamma(\mathbb{R})} \left(u' \overline{v'} - (\lambda^2 - V_a(x)) u \overline{v} \right) \mathrm{d}x \\
&= \int_\mathbb{R} \left((u' \overline{v'}) \circ x_\gamma - (\lambda^2 - V_a(x_\gamma)) (u \overline{v}) \circ x_\gamma \right) x'_\gamma \, \mathrm{d}x \\
&= \int_\mathbb{R} \left(\frac{u'_\gamma}{x'_\gamma} \frac{\overline{v'_\gamma}}{x'_\gamma} - (\lambda^2 - V_a(x_\gamma)) u_\gamma \overline{v_\gamma} \right) x'_\gamma \, \mathrm{d}x \\
&= s^S_\gamma(u_\gamma, v_\gamma).
\end{aligned}$$

We required u to be holomorphic on $O \supset \operatorname{crit}_+ x_\gamma$. If we manage to find a test function v, which is holomorphic on an open set $\widetilde{O}$ such that $O \supseteq \widetilde{O} \supset \overline{\operatorname{crit}_+ x_\gamma}$ and non-zero at p, then the integrand of (2.2.5), denoted $I_t(u, v)$, is holomorphic on $\operatorname{crit}_+ x_\gamma$ if and only if V_a is holomorphic on $\operatorname{crit}_+ x_\gamma$. The requirements for u and v to be non-zero at the pole p is essential since such a zero point could offset the pole of V, resulting in a removable singularity of $I_t(u, v)$. In the following, we will use the test function

$$w(x) = \begin{cases} \exp(-C_3 x), & 0 \leq \Re[x] \\ \exp(-C_3 x)(1 + \Re[x]), & -1 \leq \Re[x] < 0 \\ 0, & \Re[x] < -1 \end{cases},$$

with $C_3 > C_1$ as defined in Lemma 2.2.3. The restriction (2.2.3) allows direct application of this lemma. It has the desired holomorphic property and under the assumed scaling the space inclusion $w_\gamma|_{\mathbb{R}} \in H^1_\gamma(\mathbb{R})$ is easily verified. The previous lemma proves that $t_{\mathbb{R}}(u, w)$ is not only well defined, but even $t_{\mathbb{R}}(u, w) = 0$, despite $w|_{\mathbb{R}} \notin H^1_{\text{comp}}(\mathbb{R})$.

We define the following paths from the unit interval $[0, 1]$ to $\mathbb{C}$ and all $k \in \mathbb{N}$:

$$\begin{aligned}
\Gamma_{1,k}&\colon x \mapsto kx + R,\\
\Gamma_{2,k}&\colon x \mapsto x_\gamma(k(1-x) + R),\\
\Gamma_{3,k}&\colon x \mapsto \Gamma_{1,k}(1)(1-x) + \Gamma_{2,k}(0)x.
\end{aligned}$$

For any $k \in \mathbb{N}$ the concatenated path $\Gamma_k \coloneqq \Gamma_{1,k} + \Gamma_{3,k} + \Gamma_{2,k}$ is closed. Furthermore, the paths $\Gamma_{1,k}$ and $\Gamma_{2,k}$ lie on the boundary of $\text{crit}_+ x_\gamma$ (see Figure 2.2) and for any $x \in \text{crit}_+ x_\gamma$ there exists $j \in \mathbb{N}$, such that x lies in the interior of Γ_k for all $k \geq j$. Let u be a function such that *(i)* holds and assume *(i)* $\leftrightarrow$ *(ii)*. Using the residue theorem, we get

$$t_{\Gamma_k}(u, w) = \begin{cases} 2\pi i \operatorname{Res}_p I_t(u, v), & \text{if } p \text{ lies in the interior of } \Gamma_k \\ 0, & \text{otherwise} \end{cases},$$

and obtain the equivalence

$$p \notin \text{crit}_+ x_\gamma \quad \Leftrightarrow \quad \lim_{k\to\infty} t_{\Gamma_k}(u, w) = 0,$$

where w is the test function defined above.

Previous to using this condition, we show that $\lim_{k\to\infty} t_{\Gamma_{3,k}}(u, w) = 0$. Since $\lim_{|x|\to\infty} V_a(x) \to 0$ there exists $C > \left(C_3 + \max_{x\in\Gamma_{3,k}} |(\lambda^2 - V_a(x))|\right)$ independent of k and we get

$$\begin{aligned}
\lim_{k\to\infty}\left|t_{\Gamma_{3,k}}(u, w)\right| &= \lim_{k\to\infty}\left|\int_{\Gamma_{3,k}} \left(u'\overline{w'} - (\lambda^2 - V_a(x))u\overline{w}\right) \mathrm{d}x\right|\\
&= \lim_{k\to\infty}\left|\int_{\Gamma_{3,k}} \left(C_3 u' - (\lambda^2 - V_a(x))u\right) \overline{w}\, \mathrm{d}x\right|\\
&\leq \lim_{k\to\infty} \int_{\Gamma_{3,k}} C\left(|u'| + |u|\right)|w|\, \mathrm{d}x\\
&\preceq \lim_{k\to\infty} \int_{\Gamma_{3,k}} \exp(C_1 \Re[x]) \exp(C_3 \Re[x])\, \mathrm{d}x\\
&= \lim_{k\to\infty} \exp\left((C_1 - C_3)(k + R)\right) \int_{\Gamma_{3,k}} \mathrm{d}x.
\end{aligned}$$

The last equality follows from the fact that $x_\gamma(x) = x + i(x - R)$ for $x > 0$ and

$$\begin{aligned}
\Gamma_{3,k}(y) &= \Gamma_{1,k}(1)(1-y) + \Gamma_{2,k}(0)y\\
&= (k + R)(1-y) + x_\gamma(k + R)y\\
&= (k + R)(1-y) + (k + R)y + iky\\
&= (k + R) + iky,
\end{aligned}$$

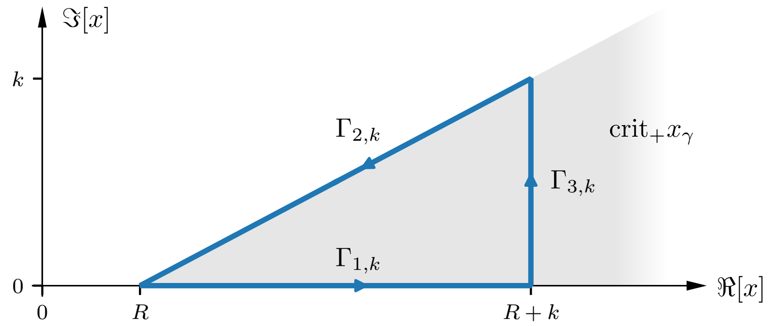

Figure 2.2: The integration paths constructed in Theorem 2.2.6.

which shows that $\Re[\Gamma_{3,k}(y)]$ is constant. Furthermore we see $\int_{\Gamma_{3,k}} \mathrm{d}x = \int_{[0,1]} \left|\Gamma'_{3,k}(x)\right| \mathrm{d}x = k$ and since $C_1 < C_3$ we get

$$\lim_{k\to\infty} \left|t_{\Gamma_{3,k}}(u,w)\right| \preceq \lim_{k\to\infty} \exp((C_1 - C_3)(k+R))k = 0, \tag{2.2.6}$$

and finally have assembled all pieces needed to show the claimed result. Since $x = x_\gamma$ for all $x \in \Omega_{\mathrm{int}}$ there holds

$$\begin{aligned} 0 &= t_{\mathbb{R}}(u,w) - t_{x_\gamma(\mathbb{R})}(u,w) \\ &= \lim_{k\to\infty} \left(t_{\Gamma_{1,k}}(u,w) + t_{\Gamma_{2,k}}(u,w)\right) \\ &= \lim_{k\to\infty} t_{\Gamma_k}(u,w). \end{aligned}$$

□

Remark 2.2.7. *The previous theorem can be generalized to other deformation functions. If τ is polynomially bounded, the proof requires only minor adaptations. Exponential deformation functions on the other hand demand for stricter constraints on the asymptotic behavior of solutions u since the quantity $\int_{\Gamma_{3,k}} \mathrm{d}x$ can no longer be easily absorbed.*

2.3 The harmonic oscillator

The harmonic oscillator represents a special case of the time-independent Schrödinger equation. Its potential function $V(x) = x^2$ is of interest to us, since it constitutes the pointwise limit of the rational potentials $V_a(x)$ we treated in the previous sections. There holds

$$\frac{x^2}{1 + \left(\frac{x}{a}\right)^4} \xrightarrow{a\to\infty} x^2, \quad x \in \mathbb{C} \tag{2.3.1}$$

This potential function has the additional key benefit that the eigenpairs of the associated Hamilton operator can be solved analytically. Its exact resonances are of the form $\sqrt{2n+1}$, $n \geq 0$.

Definition 2.3.1. *((Physicists) Hermite polynomials) The Hermite polynomials are orthogonal polynomials with respect to weight function $w(x) = e^{-x^2}$, that is to say $\int_{\mathbb{R}} w(x)H_n(x)H_m(x)\,\mathrm{d}x = \sqrt{\pi}2^n n!\delta_{n,m}$. They can be defined as*

$$H_n(x) := (-1)^n e^{x^2} \frac{\mathrm{d}^n}{\mathrm{d}x^n} e^{-x^2}.$$

Proposition 2.3.2. *The Hermite polynomials satisfy the following recurrence relations:*

(i) $H_{n+1}(x) = 2xH_n(x) - H_n'(x)$.

(ii) $H_{n+1}'(x) = 2(n+1)H_n(x)$.

Proof. The first relation is quickly confirmed:

$$\begin{aligned} H_{n+1}(x) &= -e^{x^2}\frac{\mathrm{d}}{\mathrm{d}x}\left(H_n(x)e^{-x^2}\right) \\ &= -e^{x^2}\left(H_n'(x)e^{-x^2} - 2xH_n(x)e^{-x^2}\right) \\ &= 2xH_n(x) - H_n'(x), \end{aligned}$$

whereas the second requires slightly more work. We start off with

$$\begin{aligned} (-1)^{n+1}\frac{\mathrm{d}}{\mathrm{d}x}H_{n+1}(x) &= \frac{\mathrm{d}}{\mathrm{d}x}e^{x^2}\frac{\mathrm{d}^{n+1}}{\mathrm{d}x^{n+1}}e^{-x^2} \\ &= 2xe^{x^2}\frac{\mathrm{d}^{n+1}}{\mathrm{d}x^{n+1}}e^{-x^2} + e^{x^2}\frac{\mathrm{d}^{n+1}}{\mathrm{d}x^{n+1}}(-2x)e^{-x^2} \\ &= 2xe^{x^2}\frac{\mathrm{d}^{n+1}}{\mathrm{d}x^{n+1}}e^{-x^2} + e^{x^2}\sum_{k=0}^{n+1}\binom{n+1}{k}\frac{\mathrm{d}^k}{\mathrm{d}x^k}(-2x)\frac{\mathrm{d}^{n+1-k}}{\mathrm{d}x^{n+1-k}}e^{-x^2}. \end{aligned}$$

Since $\frac{\mathrm{d}^k}{\mathrm{d}x^k}(-2x) = 0$ for $k > 1$, only the first terms of the sum in the last line are non-zero and we get

$$\begin{aligned} (-1)^{n+1}\frac{\mathrm{d}}{\mathrm{d}x}H_{n+1}(x) &= 2xe^{x^2}\frac{\mathrm{d}^{n+1}}{\mathrm{d}x^{n+1}}e^{-x^2} + e^{x^2}\left(-2x\frac{\mathrm{d}^{n+1}}{\mathrm{d}x^{n+1}}e^{-x^2} - 2(n+1)\frac{\mathrm{d}^n}{\mathrm{d}x^n}e^{-x^2}\right) \\ &= -2(n+1)(-1)^nH_n(x). \end{aligned}$$

□

Definition 2.3.3. *(Hermite functions) The Hermite functions are a sequence of orthonormal functions based on the Hermite polynomials:*

$$\psi_n(x) := (2^n n!\sqrt{\pi})^{\frac{1}{2}}e^{-\frac{x^2}{2}}H_n(x).$$

Proposition 2.3.4. *The Hermite functions are eigenfunctions of the Hamilton operator associated with the harmonic oscillator. They satisfy*

$$\psi_n''(x) + (2n+1-x^2)\psi_n(x) = 0,$$

implying eigenpairs of the form $(\psi_n, \sqrt{2n+1})$.

Proof. Since the constant term $(2^n n!\sqrt{\pi})^{1/2}$ occurs on both sides of the equation, we omit it from the proof and use the unscaled functions $\varphi_n := e^{-x^2/2}H_n$. Translating the recurrence relations of Proposition 2.3.2 to φ_n yields the relations $\varphi_{n+1} = x\varphi_n - \varphi_n'$ and $\varphi_{n+1}' = -x\varphi_{n+1} + 2(n+1)\varphi_n$, which lead to

$$\begin{aligned} 0 &= -\varphi_{n+1}' - x\varphi_{n+1} + 2(n+1)\varphi_n \\ &= -(x\varphi_n - \varphi_n')' - x(x\varphi_n - \varphi_n') + 2(n+1)\varphi_n \\ &= -\varphi_n - x\varphi_n' + \varphi_n'' - x^2\varphi_n + x\varphi_n' + 2(n+1)\varphi_n \\ &= \varphi_n'' + (2n+1-x^2)\varphi_n. \end{aligned}$$

□

Chapter 3

Numerical tests

The resonances of the discrete spectrum essentially fall into two categories, which we will refer to as *physical* and *artificial*. The first category represents the unknowns we are interested in; they are approximations to resonances of the continuous problem and will, provided that certain requirements are met (see Appendix), converge to their continuous counterpart. Artificial, also called *spurious*, resonances have no physical basis, they are artifacts introduced by the discretization of our problem.

The distinction between these categories can be difficult, as the location of the exact physical resonances is usually only roughly known – or not known at all. Furthermore, since all resonances in the discrete spectrum are afflicted by numerical errors, the role of a discrete resonance can be ambiguous even if the exact values of the continuous problem are given. In general, we can observe that coarser methods (which may refer to a larger mesh resolution parameter h, lower polynomial order p or a number of other parameters) will generate spectra in which physical and artificial resonances are less well separated. This leads to a trade-off between the computational complexity of our numerical methods and the ambiguity of the resulting resonances. We would like to compute the discrete spectrum quickly, but retain the ability to identify physical resonances. In the following sections we will analyze the influence of discretization parameters on the discrete spectrum. All conclusions drawn are to be considered with care, as they are based on numerical results and as such are approximations, and consequently falsifications. We will merely state experimental observations.

It is convenient to assign some unified notation. We write

$$V_h(x) := x^2 \quad \text{and} \quad V_a(x) = \frac{x^2}{1 + \left(\frac{x}{a}\right)^4},$$

to distinguish between potentials, where the subscript h of V_h indicates the relation to the harmonic oscillator and the parameter a might be instantiated to a fixed value (for example $V_7(x) := x^2(1 + (x/7)^4)^{-1}$). Analogous subscripts are used for the spectrum arising from the resonance problem of the time-independent Schrödinger equation of a specific potential. In particular $\sigma_h := \{ \sqrt{2n+1} : n \in \mathbb{N}_0 \}$ is the spectrum of the Hamilton operator associated with the harmonic oscillator, and σ_a^θ refers to the discrete spectrum obtained from the *numeric solution* of a resonance problem with potential $V_a(x)$. The parameter θ refers to a set of discretization parameters and might be omitted if it is clear from context or inconsequential. Note, that the inclusion of θ does not render σ_a^θ an entirely deterministic property as even with the exclusion of unavoidable numerical inaccuracies, some random elements can be introduced by certain numerical procedures. Finally, in order to refer to specific eigenpairs, we write $(\psi_{h,n}, \lambda_{h,n})$ for $\lambda_{h,n} \in \sigma_h$ and $(\psi^\theta_{a,n}, \lambda^\theta_{a,n})$ for

$$\lambda^\theta_{a,n} := \underset{\mu \in \sigma^\theta_a \setminus \{ \lambda^\theta_{a,i} : i < n \}}{\arg\min} \left| \mu - \lambda_{h,n} \right| .$$

This enumeration of numerical resonances breaks down if n is chosen too large. Nonetheless, it proves to be a useful designation in the following tests.

3.1 Invariance under discretization parameters

As physical resonances are based on some physical *ground truth*, we would expect them to be largely independent of discretization parameters as long as these parameters remain in the domain of competency of our numerical methods. The intent of the next experiment is to verify this expectation. It will serve as a basis to all following sections, as the absence of such an independence property would challenge the practicality of the entire complex scaling method. At this point we are not concerned with questions about computational efficiency.

There exists a substantial number of discretization parameters, falling essentially into four categories:

(i) Domain: The shape of the interior domain. In our one-dimensional setting it is described entirely by the parameter R.

- R: The interval size of the interior domain $\Omega_{\text{int}} = (-R, R)$.

(ii) Finite element space: $H^1(\Omega)$.

- h: Global triangulation size. It may be separated into h_{int} in the interior domain and h_{ext} in the exterior domain.
- p: Polynomial order.

(iii) Complex scaling: see (3.1.1).

- T: The numerical exterior domain is truncated to finite size with width T, resulting in $\Omega_{\text{ext}} = (-R-T, -R] \cup [R, R+T)$ and a homogeneous Dirichlet boundary condition is posed on the outer boundary $\{ \pm(R+T) \}$.
- τ: The deformation function of (3.1.1).
- α: The scaling constant of (3.1.1).

(iv) Eigenvalue solver: Arnoldi iteration.

- k: Krylov space dimension.
- s: Shift parameter.

For the experimental setup, we compute a reference spectrum with fine discretization parameters θ_{ref}. In this spectrum we identify resonances that can be classified as physical with reasonable certainty. This is done, in part, by taking the spectrum of the harmonic oscillator as a reference point and supported by their invariance in the following test. The reference spectrum is compared to resonances obtained from coarser discretization

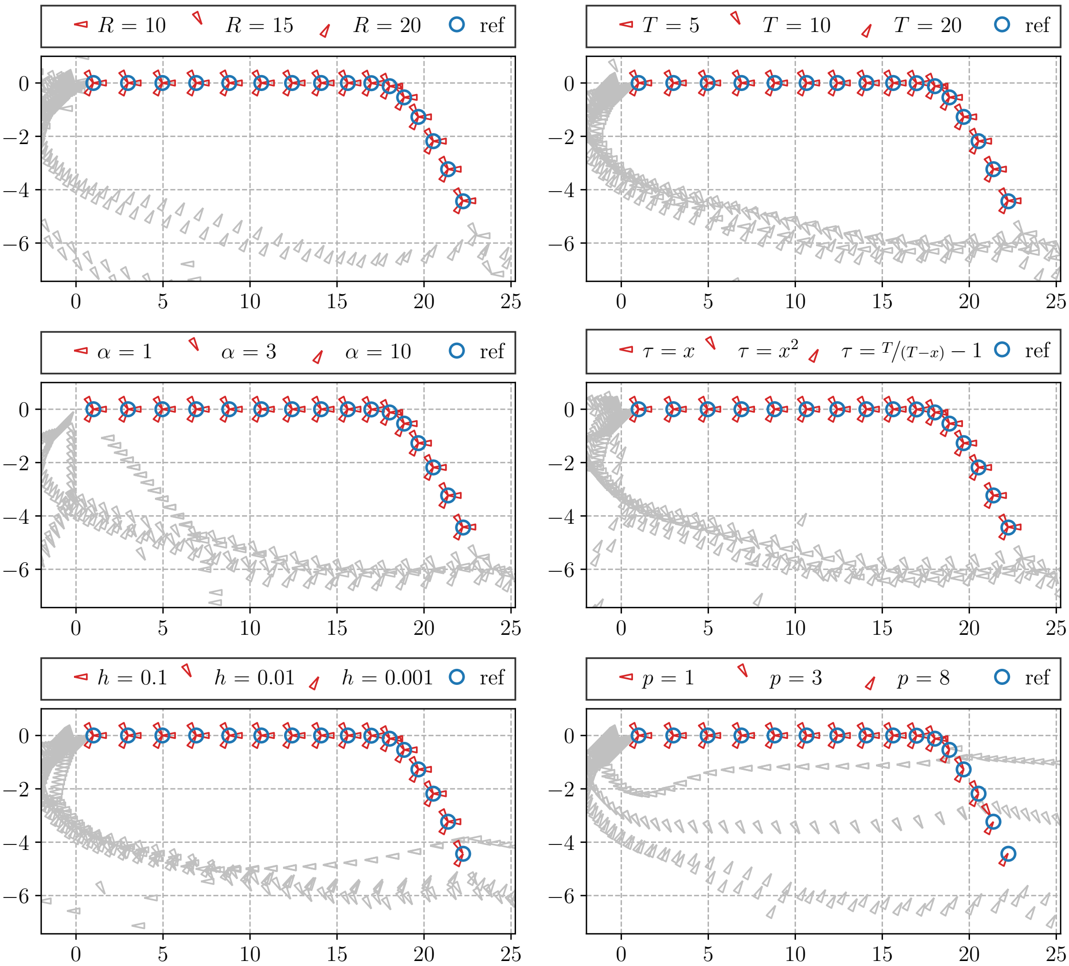

Figure 3.1: Resonances are plotted in the complex plane. Physical resonances are invariant across all discretization parameters as long as no artificial resonances (gray) exist in close proximity.

$$\theta_{\text{ref}} = \left\{ \begin{array}{ll} \text{Domain: } R = 20 & \text{Complex scaling: } T = 10, \alpha = 10, \tau(x) = x \\ \text{FE space: } h = 10^{-3}, p = 8 & \text{Solver: } \textit{Arnoldi}, k = 250, s = 20 + 0i \end{array} \right\}$$

$$\theta_{\text{base}} = \left\{ \begin{array}{ll} \text{Domain: } R = 20 & \text{Complex scaling: } T = 10, \alpha = 10, \tau(x) = x \\ \text{FE space: } h = 10^{-2}, p = 8 & \text{Solver: } \textit{Arnoldi}, k = 200, s = 20 + 0i \end{array} \right\}$$

parameters θ_{base} that have been chosen, such that the emergence of adverse effects can be provoked. Resonances that match reference values are classified as physical, and as artificial otherwise.

We test three parameters tied to the finite element space, namely the global triangulation size h, polynomial order p and the size of the interior domain R. Additionally we test three parameters of the complex scaling method: The width T of the exterior domain, the scaling parameter α and the deformation function τ which are used to form a complex scaling function

$$\gamma_{\tau,\alpha,R}(r) := \begin{cases} r & , r \in [0, R] \\ r + i\alpha\tau(r - R) & , r \geq R \end{cases} . \tag{3.1.1}$$

Parameters are varied one at a time and otherwise fixed to θ_{test}. Our test shows (see

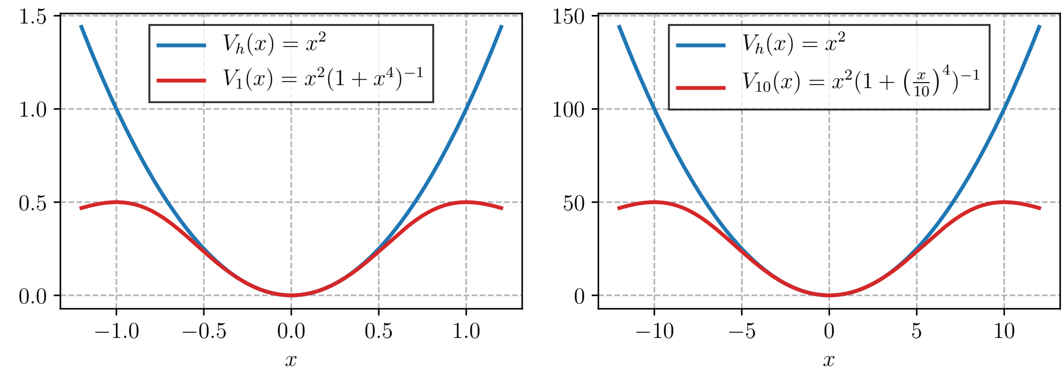

Figure 3.2: A comparison of the potentials $V_h(x)$ and $V_a(x)$ for $a = 1$ and $a = 10$.

Figure 3.1) that resonances are indeed stable across all six parameters and are only lost if artificial resonances exist in close proximity. The artificial components of the spectrum, for the most part, have clear structure and generally tend to have bigger overlap with physical resonances if discretization is more coarse.

3.2 Smooth dependence of σ_a on data

Even though the potentials $V_h(x) = x^2$ and $V_a(x) := x^2(1+({}^x\!/\!_a)^4)^{-1}$ have vastly different asymptotic behavior, they are similar within a region of approximately $(-{}^a\!/\!_2, {}^a\!/\!_2)$. As the eigenfunctions of the harmonic oscillator decay exponentially, we argue that eigenpairs (ψ_n, λ_n) are decent approximations to eigenpairs for a potential V_a for n, such that the *essential support* of ψ_n lies within a region where $V_a(x) - x^2$ is small. Since $\operatorname{supp}\psi_n = \mathbb{R}$ for all n we use the term essential support to refer to a subset of $\mathbb{R}$, where ψ_n is decidedly non-zero, such as $\operatorname{supp}_\varepsilon \psi_n := \overline{\{\, x \in \Omega : |\psi_n(x)| \geq \varepsilon \,\}}$ for some small $\varepsilon > 0$. For such n, this argument is motivated by the following estimation

$$\begin{aligned}\left\|\left(-\frac{\mathrm{d}^2}{\mathrm{d}x^2} + V_a(x)\right)\psi_n - \lambda_n\psi_n\right\|_{L^2(\mathbb{R})} &= \left\|\left(-\frac{\mathrm{d}^2}{\mathrm{d}x^2} + V_a(x) + x^2 - x^2\right)\psi_n - \lambda_n\psi_n\right\|_{L^2(\mathbb{R})} \\ &\leq \left\|(V_a(x) - x^2)\psi_n\right\|_{L^2(\mathbb{R})} \qquad (3.2.1) \\ &\leq \max_{x\in\operatorname{supp}_\varepsilon\psi_n}(V_a(x) - x^2) + \left\|(V_a(x) - x^2)\psi_n\right\|_{L^2(\mathbb{R}\setminus\operatorname{supp}_\varepsilon\psi_n)}.\end{aligned}$$

The property $\|\psi_n\|_{L^2(\mathbb{R})} = 1$ simplifies the first term in the last line and the second term is small for the chosen n.

If we assume smooth dependence of eigenvalues and eigenfunctions on the potential V, then it is not unreasonable to expect a similarity between the spectrum of the harmonic oscillator with potential $V_h(x)$ and the time-independent Schrödinger equation with bounded potentials $V_a(x)$. We can observe the claimed similarities of eigenvalues in Figure 3.3. For larger n, the eigenvalues $\lambda_{a,n}$ corresponding to $V_a(x)$ tend to have a smaller real component and will eventually exhibit a significant imaginary component.

The following examples show how the magnitude of $\Im[\lambda_{a,n}]$ plays a major role in the asymptotic behavior of their corresponding eigenfunctions.

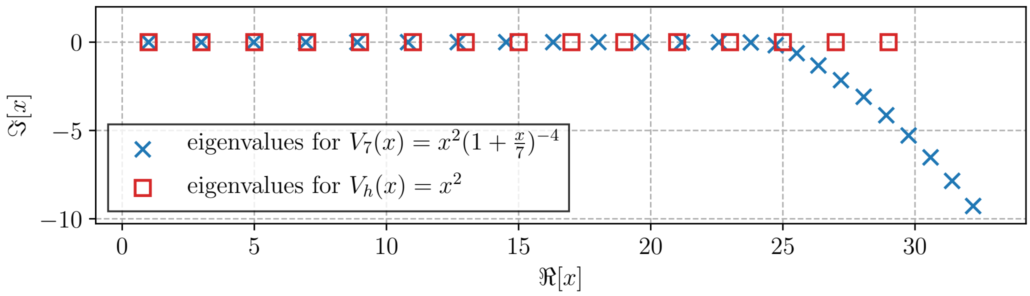

Figure 3.3: A numerical comparison of eigenvalues for the potentials $V_h(x)$ and $V_a(x)$ for small n.

Example 3.2.1. *We compare the eigenfunctions $\psi_{h,5}$ and $\psi^{\theta}_{a,5}$ with the corresponding eigenvalues $\lambda_{h,5} = 11$ and $\lambda^{\theta}_{a,5} = 10.22 - 1.18 \times 10^{-4} i$ for the potential parameter $a = 5$ (see Figure 3.4 for parameters θ).*

We note a distinct reduction of $\Re[\lambda_{a,5}]$ compared to $\lambda_{h,5}$ whereas $\Im[\lambda_{a,5}]$ is small. This is consistent with our observations of Figure 3.3. We have previously argued that there is a connection between similarity of eigenfunctions $\psi_{h,n}$ and $\psi_{a,n}$ and their essential support in relation to $|V_h(x) - V_a(x)|$. In this particular example, the essential support of $\psi_{h,5}$ closely resembles the interval between the two maxima of $V_a(x)$. Since $\arg\max_{x \in \mathbb{R}} V_a(x) = a$ we have $\operatorname{supp}_{\varepsilon} \psi_{h,5} \sim (-a, a)$ which exceeds the previously suggested region $(-{}^a/_2, {}^a/_2)$ within which $|V_h(x) - V_a(x)|$ is small. Figure 3.4 shows notable differences between the two eigenfunction, although their general shape and asymptotic behavior is similar. Small oscillations are discernible in the asymptotic behavior of $\psi_{a,5}$ that are absent in $\psi_{h,5}$. //

Example 3.2.2. *We compare the eigenfunctions $\psi_{h,6}$ and $\psi^{\theta}_{a,6}$ with the corresponding eigenvalues $\lambda_{h,6} = 13$ and $\lambda^{\theta}_{a,6} = 11.63 - 1.24 \times 10^{-2} i$ for the potential parameter $a = 5$ (see Figure 3.5 for parameters θ).*

The setting of this example is identical to Example 3.2.1 and we have moved to the next eigenpair in line. At this point the eigenvalues $\lambda_{h,n}$ and $\lambda_{a,n}$ diverge more severely. We have $\Re[\lambda_{h,6} - \lambda_{a,6}] = 1.37$ compared to $\Re[\lambda_{h,5} - \lambda_{a,5}] = 0.78$ and, perhaps more significantly, $|\Im[\lambda_{a,6}]|$ has increased by two orders of magnitude. Consequently, the deviation of eigenfunctions in Figure 3.5 is more pronounced and the asymptotic behavior of $\psi_{a,6}$ shows persistent oscillation. Interestingly, the increase in the essential support of $\psi_{h,6}$ compared to $\psi_{h,5}$ is very minor. More refined tests will be needed to argue for the significance of this property. //

In order to further support our claim that σ_a continuously depends on the potential $V_a(x)$ and the parameter a in particular, we study σ_a as a function of a. The limits of this function are a consequence of

$$\lim_{a \to \infty} V_a(x) = V_h(x), \quad x \in \mathbb{R},$$

and

$$\lim_{a \to 0} V_a(x) = 0, \quad x \in \mathbb{R}.$$

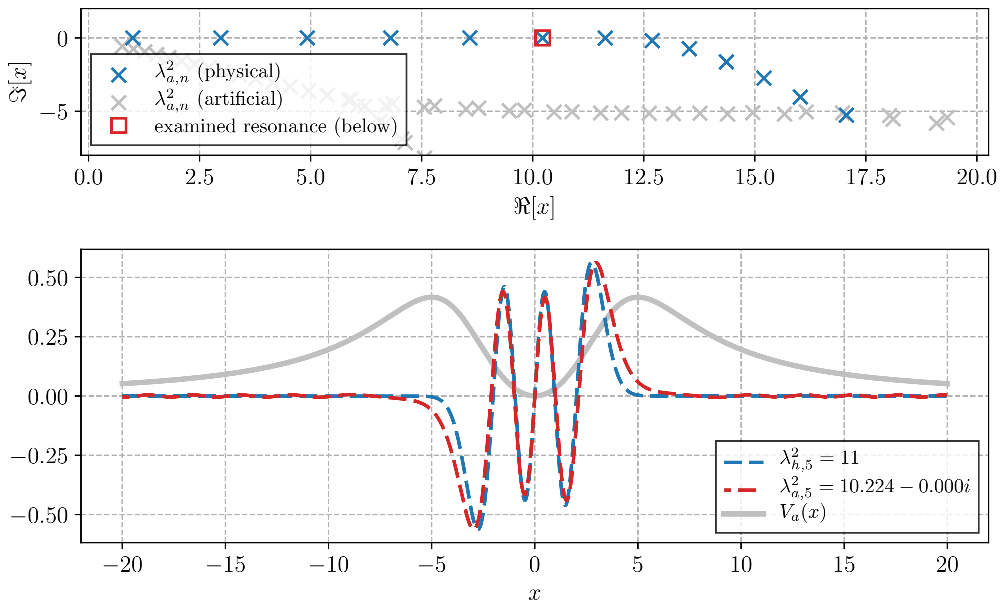

Figure 3.4: Comparison of a single eigenfunction $\psi_{h,5}$ of the harmonic oscillator $V_h(x) = x^2$, corresponding to the eigenvalue $\lambda^2_{h,5} = 11$, and the eigenfunction $\psi_{a,5}$ arising from the rational potential $V_a(x) = x^2(1 + (x/a)^4)^{-1}$ with $a = 5$.

$$\theta = \left\{ \begin{array}{ll} \text{Domain: } R = 20 & \text{Complex scaling: } T = 10, \alpha = 1, \tau(x) = x \\ \text{FE space: } h = 10^{-2}, p = 8 & \text{Solver: } \textit{Arnoldi}, k = 200, s = 10 + 0i \end{array} \right\}$$

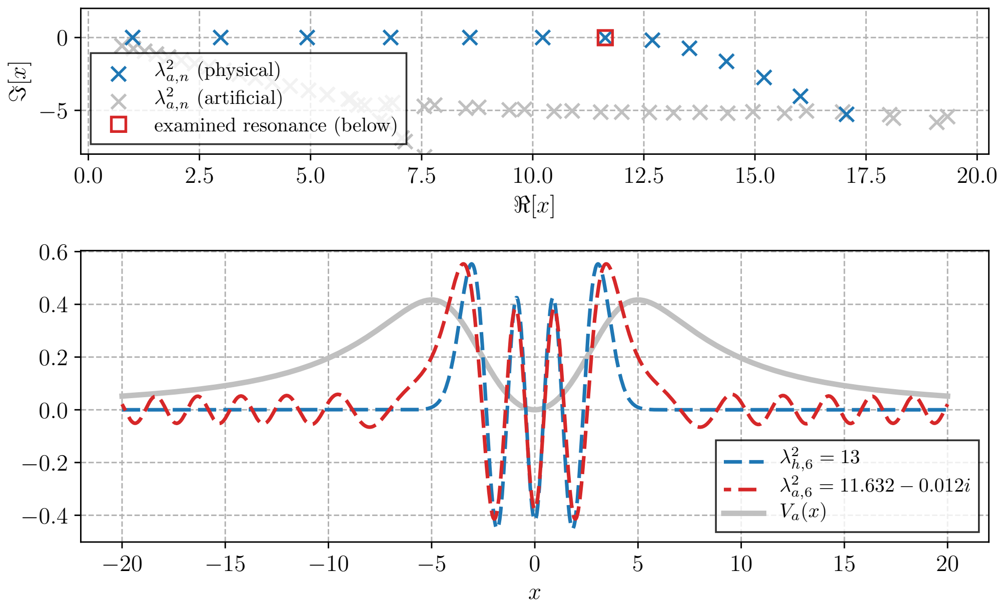

Figure 3.5: Comparison of a single eigenfunction $\psi_{h,6}$ of the harmonic oscillator $V_h(x) = x^2$, corresponding to the eigenvalue $\lambda^2_{h,6} = 13$, and the eigenfunction $\psi_{a,6}$ arising from the rational potential $V_a(x) = x^2(1 + (x/a)^4)^{-1}$ with $a = 5$.

$$\theta = \left\{ \begin{array}{ll} \text{Domain: } R = 20 & \text{Complex scaling: } T = 10, \alpha = 1, \tau(x) = x \\ \text{FE space: } h = 10^{-2}, p = 8 & \text{Solver: } \textit{Arnoldi}, k = 200, s = 10 + 0i \end{array} \right\}$$

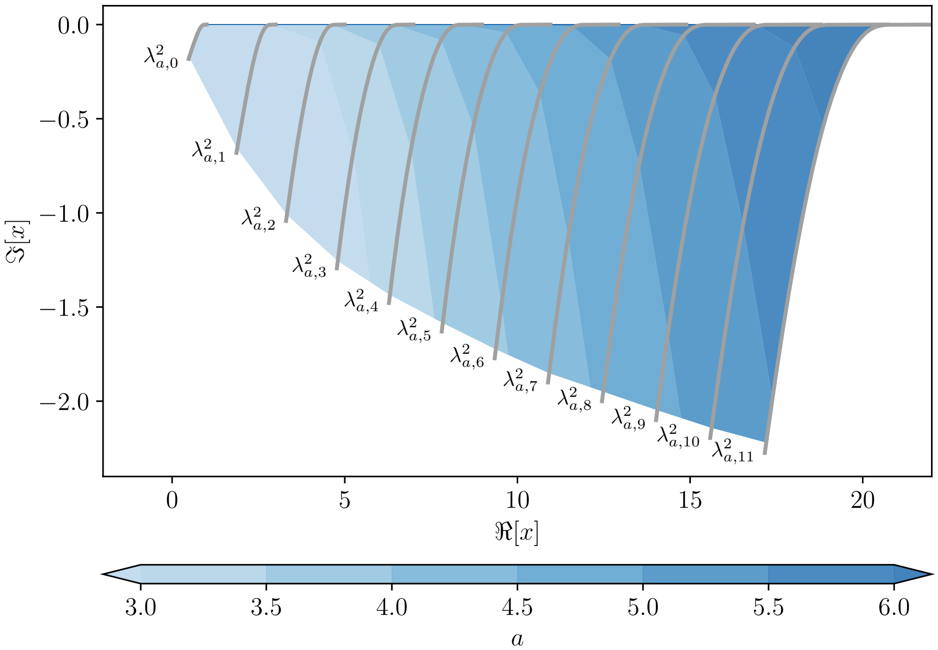

Figure 3.6: The shape of the paths $\gamma_n(a) = \lambda^2_{a,n}$ for the first 12 resonances.

As such, we expect $\gamma_n(a) \coloneqq \lambda^2_{a,n}$ to form a continuous path that approaches $\lambda^2_{h,n}$ for large a. For $a \to 0$, on the other hand, the Hamilton operator simplifies to the second order differential operator $-\frac{\mathrm{d}^2}{\mathrm{d}x^2}$ with spectrum $\mathbb{R}$ and the convergence of discrete eigenvalues is no longer guaranteed. This change will manifest itself in the form of numerical errors in our tests and the previously shown invariance of resonances under discretization parameters will be lost. We counteract this problem by performing multiple computations under different parameter sets θ. Sections of γ_n that remain invariant under these variations are assumed to be undistorted. The results of this computation for the first 12 resonances are shown in Figure 3.6 and confirm our expectations with respect to smoothness. The overall shape of the paths is similar across all n, although large changes are induced by different intervals of a. We will investigate values of a as a function of n. Specifically we are interested in a mapping $n \mapsto \{\, a : \Im[\gamma_n(a)] = c \,\}$ for some fixed $c > 0$. In our example these values of a are unique and we will use the expression

$$n \mapsto \Im[\gamma_n]^{-1}(c), \qquad (3.2.2)$$

instead. The inverse is only well defined if $\Im[\gamma_n(a)]$ is strictly monotonous. Although we cannot prove such a property in a general form, it will hold all cases treated here. The same is true for the mapping $n \mapsto \Re[\gamma_n]^{-1}(c)$. For the computed data of Figure 3.6 and fixed c the mapping (3.2.2) seems to be almost linear.

In Figure 3.7 we take a closer look at a single path γ_n for $n = 5$. It shows more clearly, that the paths γ_n are virtually constant for large a, and the deviation $\Im[\lambda^2_{a,5} - \lambda^2_{h,5}]$ is much more rapid than the real component $\Re[\lambda^2_{a,5} - \lambda^2_{h,5}]$. We would like to find a good criterion to predict the value of a at which a potential $V_a(x)$ will cause large imaginary components of $\lambda^2_{a,n}$. The bottom portion of Figure 3.7 suggests a correlation between

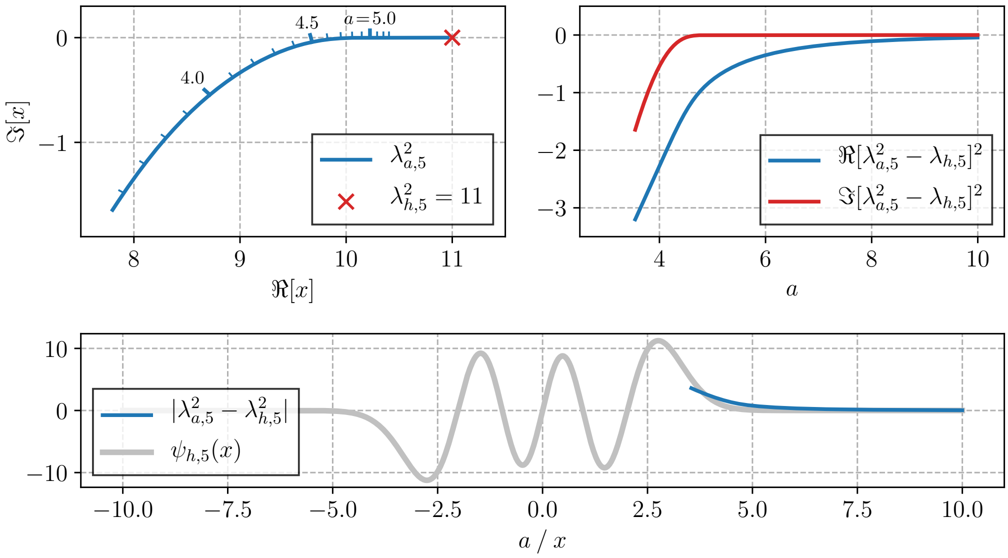

Figure 3.7: A more detailed visualization of the path $\gamma_5(a) = \lambda^2_{a,5}$ *(top)* and a comparison of the difference $\left|\lambda^2_{a,5} - \lambda^2_{h,5}\right|$ as a function of a and $\operatorname{supp}_\varepsilon \psi_{h,5}$ *(bottom)*.

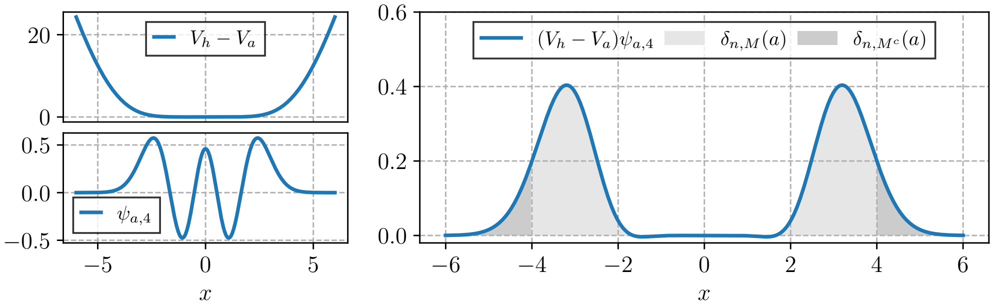

Figure 3.8: An illustration of the quantity $\delta_{n,M}(a)$ with parameters $n = 4$ and $a = 5$.

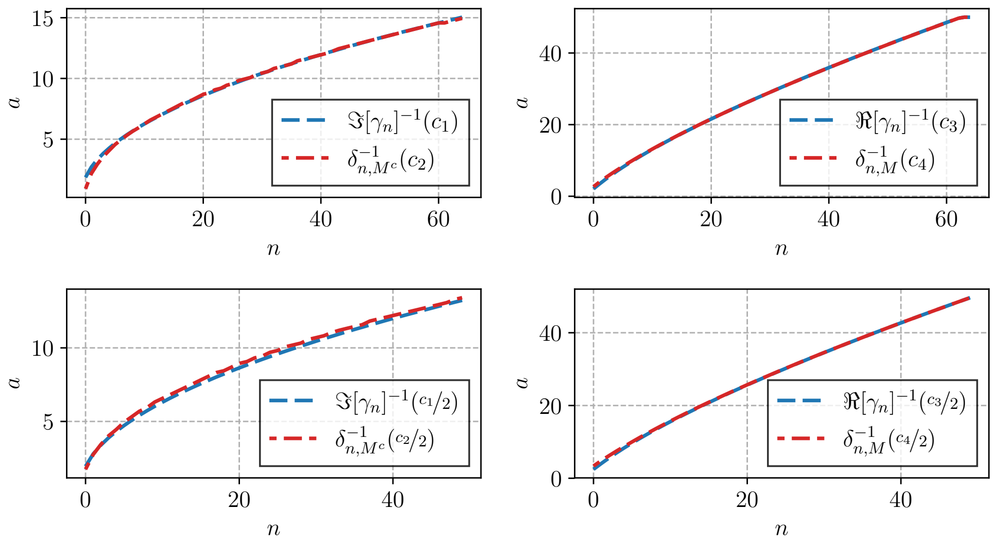

Figure 3.9: An illustration of the correlation of the quantities $\Im[\gamma_n]^{-1}(c_1)$ and $\delta^{-1}_{n,M^c}(c_2)$, as well as $\Re[\gamma_n]^{-1}(c_3)$ and $\delta^{-1}_{n,M}(c_4)$, and the independence of this property under scaling of the vector of constants $c = (0.01, 1, 0.1, 0.152)^\top$. $M(a) = (-0.8a, 0.8a)$ and $M^c(a) = \mathbb{R} \setminus (-0.8a, 0.8a)$.

$|\psi_{a,n}|$ and $|\lambda_{a,n}^2 - \lambda_{h,n}^2|$. However, as the point evaluation of $|\psi_{a,n}|$ is not monotonous, we use instead the integrated quantity (see also estimation (3.2.1))

$$\delta_{n,M}(a) := \left\| \left(V_h(x) - V_a(x)\right) \psi_n(x) \right\|_{L_2(M(a))}, \tag{3.2.3}$$

where $M(\cdot)$ maps to subsets of $\mathbb{R}$. Using the empirically chosen constants $c = (0.01, 1, 0.1, 0.152)^\top$, $M(a) = (-0.8a, 0.8a)$ and $M^c(a) = \mathbb{R} \setminus (-0.8a, 0.8a)$ we compare

$$\left(n \mapsto \Im[\gamma_n]^{-1}(c_1),\ n \mapsto \delta_{n,M^c}^{-1}(c_2)\right),$$

and

$$\left(n \mapsto \Re[\gamma_n]^{-1}(c_3),\ n \mapsto \delta_{n,M}^{-1}(c_4)\right).$$

We find, that the mapping $n \mapsto \delta_{n,M}^{-1}(c), c > 0$ is highly correlated with mapping (3.2.2) across a wide range of n. Figure 3.9 demonstrates, that this correlation remains almost entirely stable if the vector of constants c is scaled, and confirms that knowledge of an eigenfunction $\psi_{a,n}$ (or knowledge of its essential support) can be a (rough) predictor of $\Im[\lambda_{a,n}^2]$ and $\Re[\lambda_{h,n}^2 - \lambda_{a,n}^2]$.

These correlations are not unexpected, since quantum wave functions of higher energies are more likely to surpass to potential well of $V_a(x)$ which is reflected in higher magnitude of the eigenfunction $\psi_{a,n}$ outside of $(-a, a)$. The outward travel of these waves is synonymous with the transport of energy away from the origin, and the rate of decrease in energy is reflected in the imaginary component of $\lambda_{a,n}^2$.

3.3 Poles in the critical region of x_γ

3.3.1 Examples

The potential $V_a(x) = x^2 \left(1 + (x/a^4)\right)^{-1}$ has four poles p_i at $\frac{a}{\sqrt{2}}(\pm 1 \pm i)$. Theorem 2.2.6 shows that, under the assumption of some technical conditions, a proposed equivalence between the solutions of the treated scaled and unscaled variational formulations cannot hold if any pole p_i lies within the critical region of x_γ. The following numerical tests illustrate this effect. We use parameters $a = 6$ and the linear complex scaling

$$\gamma_{\tau,\alpha,R}(r) := \begin{cases} r & , r \in [0, R] \\ r + i\alpha(r - R) & , r > R \end{cases}, \tag{3.3.1}$$

and vary both the scaling parameter α (see Figure 3.10) and the size of the interior domain $\Omega_{\text{int}} = (-R, R)$ (see Figure 3.11) individually.

The metric chosen to indicate the failure of our numerical methods works as follows: A reference set of resonances is computed, of which the 15 physical resonances of smallest magnitude are stored. All subsequently computed sets of resonances are then compared with the 15 stored reference values by counting how many of them could still be computed while disregarding negligible differences. This number is denoted $n_\lambda(\alpha)$ and $n_\lambda(R)$ respectively. Our tests show indeed a sharp drop in $n_\lambda(\cdot)$ as poles

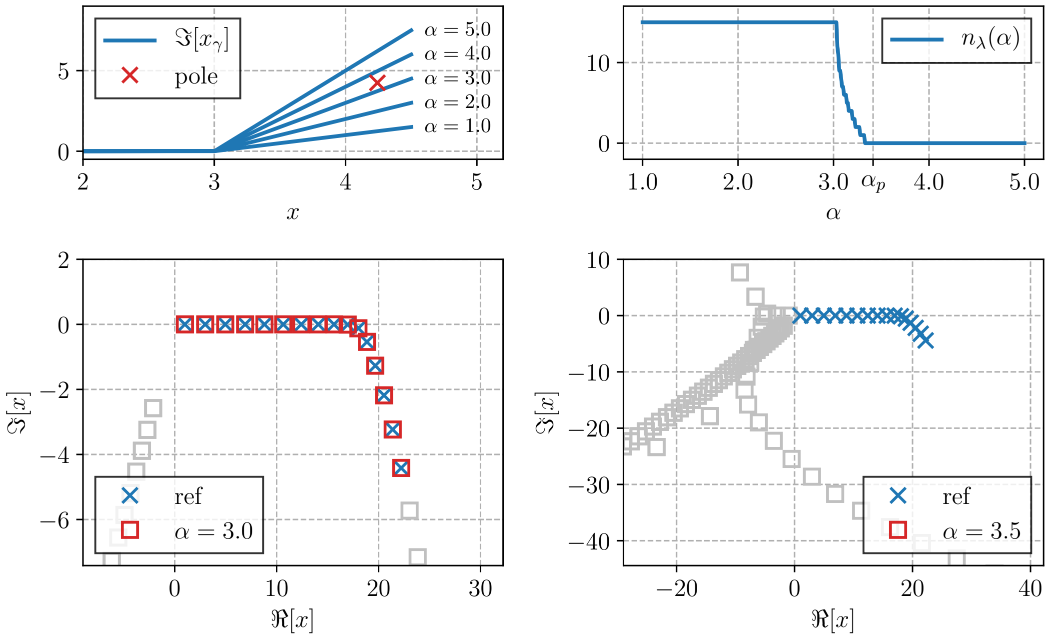

Figure 3.10: Scaling profiles with a varying scaling constant α *(top left)*. The number of resonances matching precomputed reference values $n_\lambda(\alpha)$. For $\alpha = \alpha_p$ a pole lies directly on the boundary of crit x_γ *(top right)*. Computed eigenvalues without poles in crit x_γ *(bottom left)*. Computed eigenvalues with poles in crit x_γ *(bottom right)*.

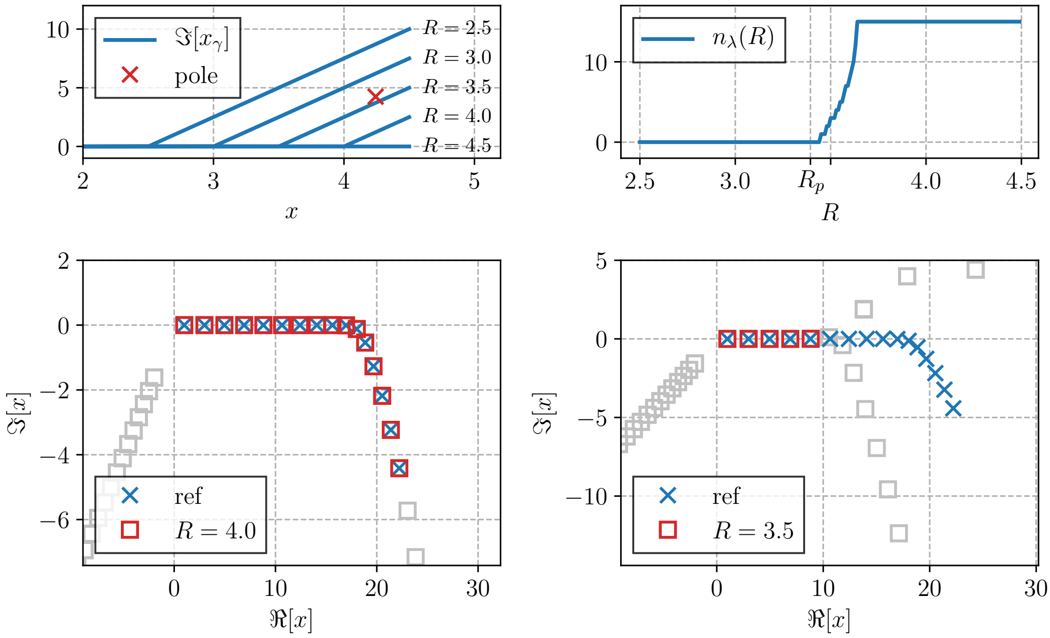

Figure 3.11: Scaling profiles with a varying interior domain size $\Omega_{\text{int}} = (-R, R)$ *(top left)*. The number of resonances matching precomputed reference values $n_\lambda(R)$. For $R = R_p$ a pole lies directly on the boundary of crit x_γ *(top right)*. Computed eigenvalues without poles in crit x_γ *(bottom left)*. Computed eigenvalues with poles in crit x_γ *(bottom right)*.

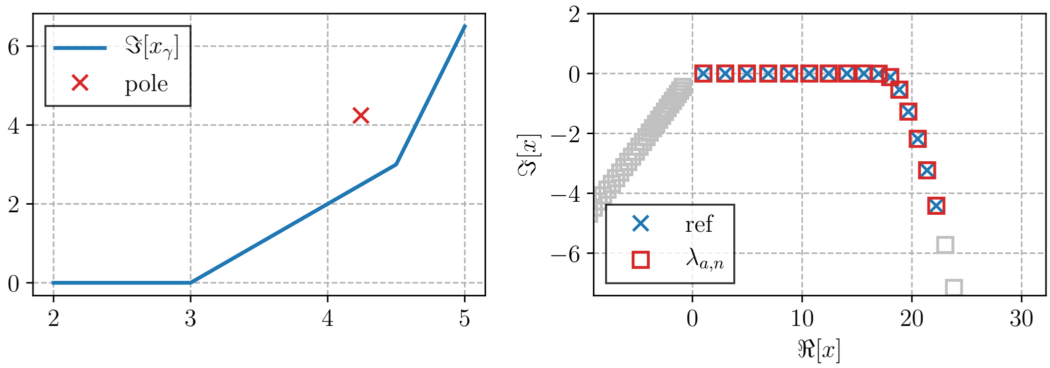

Figure 3.12: Two stacked linear scaling functions *(left)*. The corresponding discrete eigenvalues and reference values *(right)*.

approach crit x_γ, and a constant value of zero if a poles lies in the interior of crit x_γ. If finer discretization parameters are chosen, the shape of $n_\lambda(\cdot)$ approaches that of a step function.

For our particular choice of potential functions $V_a(x)$ this effect puts an interesting constraint on the choice of deformation functions. The proof of Theorem 2.2.6 has shown that one of the poles which might potentially lie within crit x_γ is $p(a) = \frac{a}{\sqrt{2}}(1+i)$. In a case where a scaling profile, which is suitable independently of the parameter a is required, the condition $p(a) \notin \operatorname{crit} x_\gamma$, $\forall a > 0$ would have to hold. Some elementary considerations show that this condition is not satisfied if $\liminf_{x\to\infty} \alpha\tau'(x) > 1$. Examples of such scaling profiles are the linear scaling used above if $\alpha > 1$, or monomials $\tau(x) = x^k$ with $k > 1$.

3.3.2 Stacked complex scaling

Stacked complex scaling profiles can be used to maximize scaling around poles in order to enable earlier truncation. For n deformation functions and scaling constants (τ_i, α_i), $1 \le i \le n$ and values $R_n \le \ldots \le R_1 = 0$ the sum

$$\tau(x) = \sum_{i=1}^{n} \alpha_i \tau_i(\max(x - R_i, 0)),$$

creates a new scaling profile. It inherits the regularity of the deformation functions τ_i in all points $x \neq R_i$.

3.4 Analysis of artificial resonances

We will test the influence of discretization parameters on artificial resonances. A good understanding of these effects can reduce computational effort tremendously. Our tests vary individual discretization parameters and compare the results to reference values. A more detailed analysis can be found in [NW18].

All tests were performed with a fixed potential $V_a(x)$ with fixed scaling parameter $a = 6$. The used reference values are resonances which remain invariant under two separate sets of fine discretization parameters

$$\theta_{\text{ref}_1} = \left\{ \begin{array}{ll} \text{Domain: } R = 5 & \text{Complex scaling: } T = 15, \alpha = 1, \tau(x) = x \\ \text{FE space: } h = 1 \times 10^{-2}, p = 10 & \text{Solver: } \textit{Arnoldi}, k = 250, s = 5 + 0i \end{array} \right\}$$

$$\theta_{\text{ref}_2} = \left\{ \begin{array}{ll} \text{Domain: } R = 5 & \text{Complex scaling: } T = 10, \alpha = 2, \tau(x) = x \\ \text{FE space: } h = 3 \times 10^{-3}, p = 8 & \text{Solver: } \textit{Arnoldi}, k = 250, s = 5 + 0i \end{array} \right\}.$$

In order to provoke visible changes in the discrete spectrum, we utilize an additional, coarser discretization baseline

$$\theta_{\text{base}} = \left\{ \begin{array}{ll} \text{Domain: } R = 5 & \text{Complex scaling: } T = 15, \alpha = 1, \tau(x) = x \\ \text{FE space: } h = 10^{-1}, p = 3 & \text{Solver: } \textit{Arnoldi}, k = 250, s = 10 + 0i \end{array} \right\}. \tag{3.4.1}$$

In each of the Figures 3.13 to 3.17 one of these parameters is varied while the others remain fixed. Resonances matching reference values are marked in blue. All other values are considered artificial and marked in gray.

The computed data shows a general and unsurprising trend: Fewer physical eigenvalues are retained if parameters are chosen more coarse. Since the distributions of both physical and artificial resonances have mostly clear structure, it might be tempting to classify all values on a *path* as either physical or artificial. Such an approach would fail in instances such as the case $T = 2$ in Figure 3.16. Furthermore, the coarsest instances $h_{\text{int}} = 1$ of Figure 3.13, $p = 1$ of Figure 3.14 and $h_{\text{ext}} = 1$ of Figure 3.15 show artificial resonances at $\Re[z] > 20$ seemingly approaching the real axis. These values might be mistaken for a continuation of physical resonances.

Some of the most striking effects are the consequence of a varying scaling parameter α and shown in Figure 3.17. Fortunately, it is possible to assign meaning to some of the artificial structures. In homogeneous exterior domains we can find radiating solutions to Helmholtz-type equations. These have the form

$$u_{\text{ext}}(x) = \begin{cases} C_1 \exp(i\omega(x - R)) & , x \in \Omega_{\text{ext}}^+ \\ C_2 \exp(-i\omega(x + R)) & , x \in \Omega_{\text{ext}}^- \end{cases},$$

as stated in Definition 1.2.1. According to Proposition 1.5.3 these solutions decay exponentially if $\alpha > -\frac{\Im[\omega]}{\Re[\omega]}$. As such, the line $\{ z \in \mathbb{C} : -\frac{\Im[z]}{\Re[z]} = \alpha \}$ or equivalently $\{ z \in C : -\arg(z) = \arctan\big(-\frac{\Im[z]}{\Re[z]}\big) = \arctan(\alpha) \}$ has significance to these solutions. Since our potential $V_a(x)$ approaches zero for large $|x|$, it seems that this significance is transferred in part to inhomogeneous exterior domains. As our tests show squared resonances, we are interested in the line $\{ z \in C : -\arg(z) = 2\arctan(\alpha) \}$. Indeed, all tests of this section with fixed $\alpha = 1$ show a structure at $\Im[z] < -40$ at an angle of roughly $-\frac{\pi}{2} = -2\arctan(1)$. Similar structures, but with varied angles roughly matching this hypothesis, can be observed in Figure 3.17.

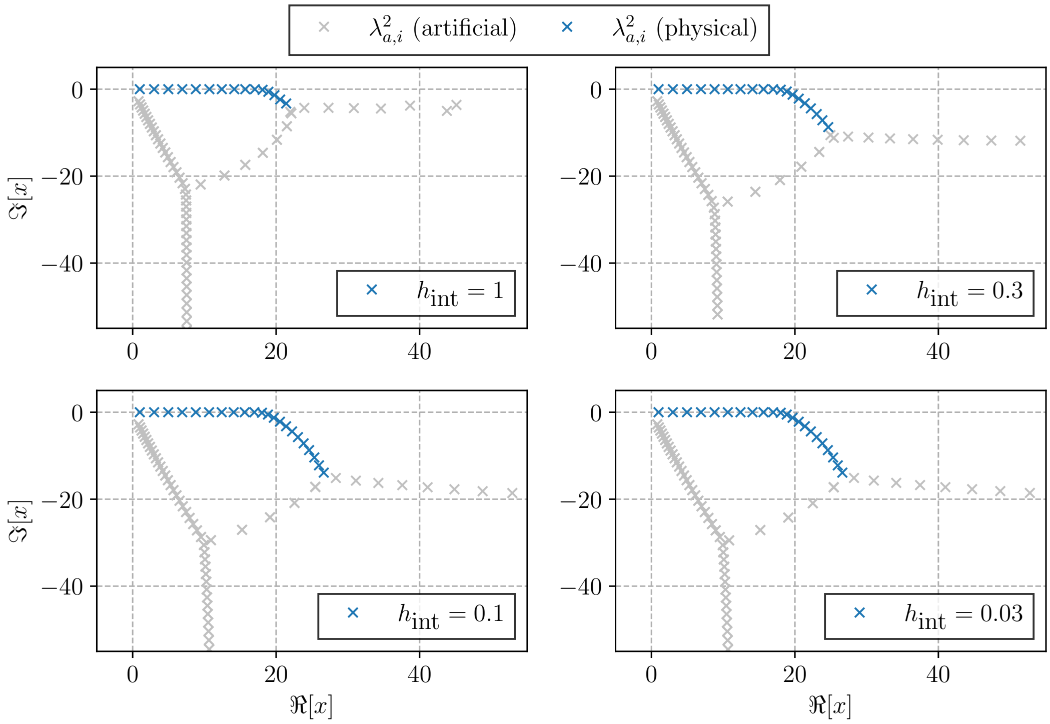

Figure 3.13: Variation of the interior triangulation size h_{int} from the baseline (3.4.1).

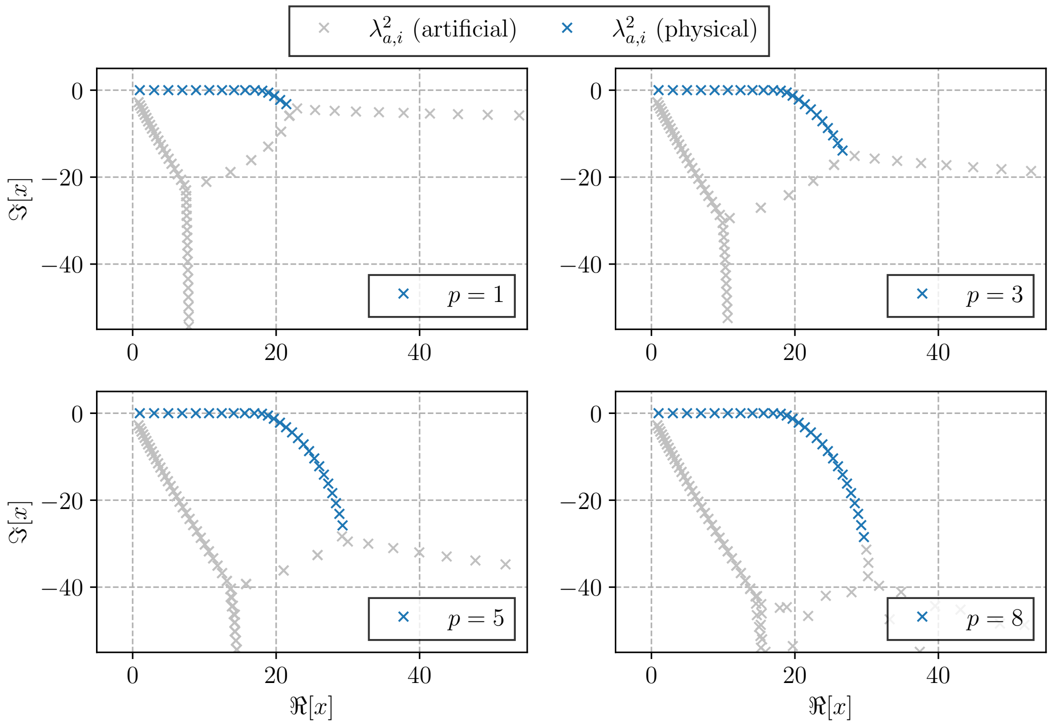

Figure 3.14: Variation of the finite element space polynomial order p from the baseline (3.4.1).

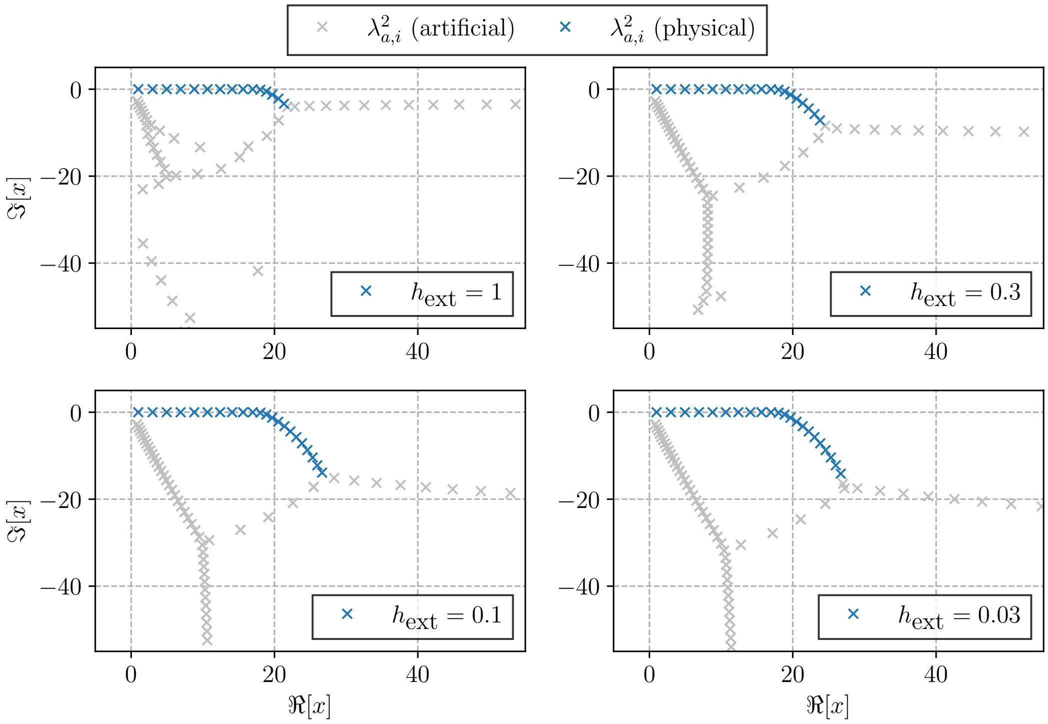

Figure 3.15: Variation of the exterior triangulation size h_{ext} from the baseline (3.4.1).

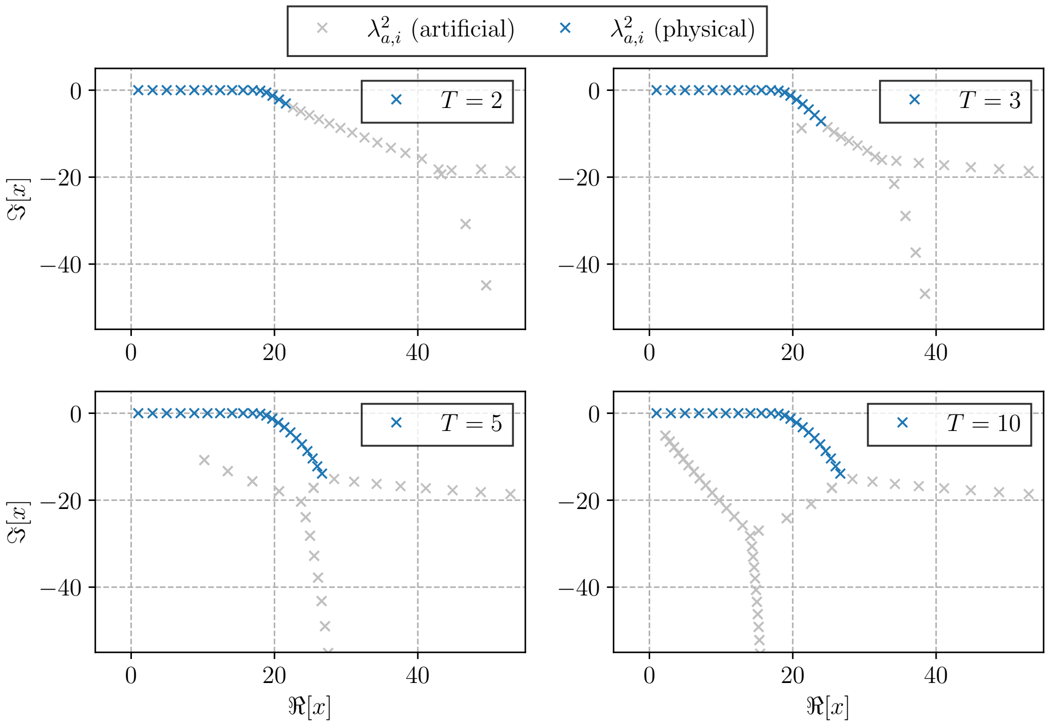

Figure 3.16: Variation of the truncation point T with $\Omega_{\text{ext}} = (-T - R, -R] \cup [R, R + T)$ from the baseline (3.4.1).

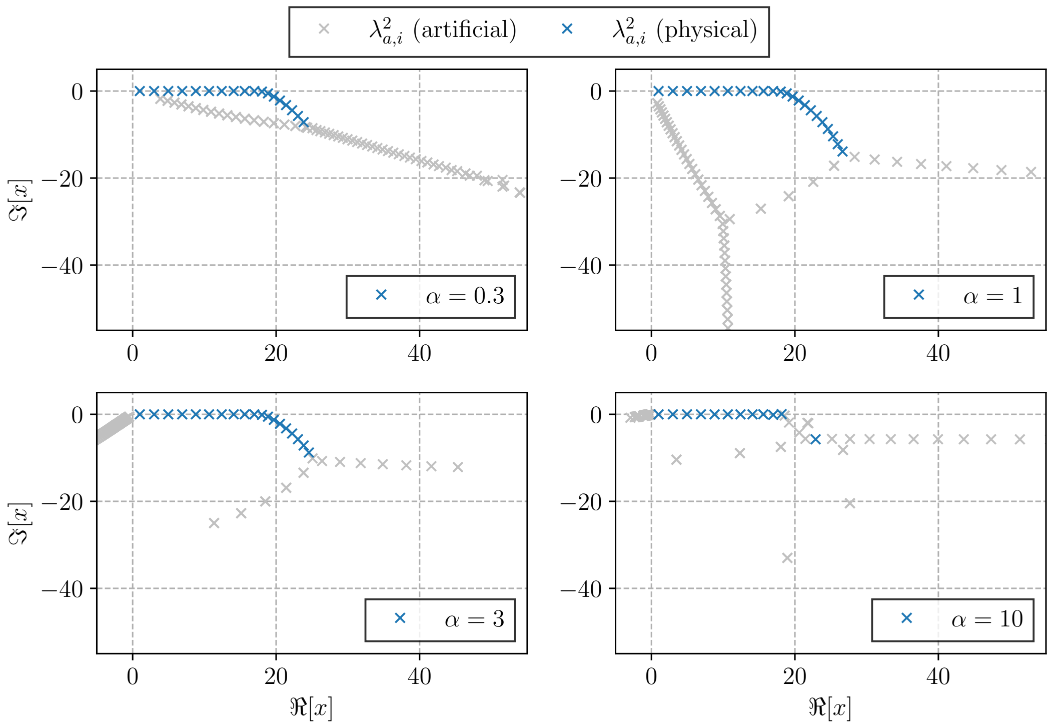

Figure 3.17: Variation of the scaling parameter α from the baseline (3.4.1).

Chapter 4

Conclusion

4.1 Summary

This thesis presented the complex scaling method in one dimension. The theoretical basis for Helmholtz-type equations with homogeneous exterior domains, as discussed in [Nan16], was generalized to a wider range of scaling profiles which led to the concept of deformation functions. An equivalence of radiating solutions and scaled solutions was proven. This makes the complex scaling method well suited for the numerical treatment of resonance problems with advantages including the exponential decay of scaled solutions in space and a linear eigenvalue structure of the complex scaled problem formulation. The second chapter further extended the method to the time-independent Schrödinger equation with inhomogeneous potential functions in the exterior domain. In this setting, the notion of radiation conditions was adapted and the previous proof, concerning equivalence of radiating solutions and scaled solutions, was weakened to necessary conditions that are mainly focused on the need for holomorphic potential functions in a so called critical region. Numerical tests were set up to study resonance problems of a family of quadratically decaying potential functions V_a and compared to an analytically known limit for $a \to \infty$. Further tests illustrated the separability of physical and artificial resonances across a range of discretization parameters. The comparatively large number of such parameters is one of the disadvantage of the complex scaling method, as the choice of computationally efficient and well behaved parameters is a time consuming task.

4.2 Future work

All results presented in this thesis are restricted to one dimension. Most practical applications however, require methods in two or three dimensions. Hence, an according extension to higher dimensions is a natural next step.

Our results concerning the equivalence of radiating and scaled solutions were satisfactory in the first chapter but had to be weakened to necessary conditions in the second. The main obstacle preventing a stronger result is the lack of explicit knowledge of solutions in the exterior domain. Based on numerical test it is conjectured that the posed conditions might already be sufficient.

Appendix

In this chapter we list important definitions and theorems. The contents of the second section are taken from [Nan16].

A Basic compact operators

Theorem A.1. *(Scalar trace operator) There exists a well defined and continuous operator*

$$Tr\colon H^1((0,1)) \to \mathbb{C},$$

whose restriction to $C^1([0,1])$ coincides with

$$u \mapsto u(0).$$

Proof. See [Sch09]. □

Theorem A.2. *(Trace operator) There exists a well defined and continuous operator*

$$Tr\colon H^1(\Omega) \to L^2(\partial\Omega),$$

which coincides with $u|_{\partial\Omega}$ for $u \in C^1(\overline{\Omega})$.

Proof. See [Sch09]. □

Definition A.3. *An operator $T\colon V \to W$ between normed spaces V and W is called compact if for any bounded sequence $(v_n)_{n\in\mathbb{N}}$ in V the sequence $(Tv_n)_{n\in\mathbb{N}}$ in W contains a convergent subsequence.*

Any continuous operator with finite rank is compact as an immediate consequence of Bolzano-Weierstrass.

For any open subset Ω of $\mathbb{R}^n$ and $m \in \mathbb{N}_0, p \geq 1$ we write $W^{m,p}(\Omega)$ to denote the Sobolev spaces of functions $f \in L^p(\Omega)$, such that for any multiindex α with $|\alpha| \leq m$ the weak derivative $D^\alpha f$ lies in $L^p(\Omega)$. The norm on this space is defined as

$$\|f\|_{m,p,\Omega} = \left(\sum_{|\alpha|\leq m} \|D^\alpha f\|_p^p \right)^{1/p}, \tag{A.1}$$

for $1 \leq p < \infty$ and

$$\|f\|_{m,\infty} = \max_{\alpha\leq m} \|D^\alpha f\|_\infty ,$$

otherwise. There holds $H^m(\Omega) = W^{m,2}(\Omega)$.

Theorem A.4. *(Rellich-Kondrachov) Let Ω be a bounded, convex, and open subset of $\mathbb{R}^n$. For every $1 \leq p \leq \infty$, the Sobolev space $W^{1,p}(\Omega)$ is compactly embedded in $L^p(\Omega)$.*

Proof. See [Eva10]. □

B Coercive operators with compact perturbations.

Theorem B.1. *(Riesz) Let $S : X \to Y$ be a bounded, linear operator with a bounded inverse $S^{-1} : Y \to X$ and $K : X \to Y$ a compact, linear operator mapping a normed linear space X to a normed linear space Y. If the homogeneous equation*

$$(S - K)\,\varphi = 0$$

has only the trivial solution $\varphi = 0$, then the inhomogeneous equation

$$(S - K)\,\varphi = f$$

has a unique solution for all $f \in X$, and $\varphi \in Y$ is continuous in f.

Proof. See [Kre99]. □

The significance of Riesz-Fredholm theory lies in the fact that it allows to reduce questions about the existence of solutions to an inhomogeneous problem, to the verification that the homogeneous equation has no non-trivial solutions.

Definition B.2. *(Orthogonal projection) Let $(V, (\cdot,\cdot)_V)$ be a Hilbert space and $X \subset V$ a closed subspace. For each fixed $u \in V$ the orthogonal projection of u onto X is defined as the unique element $v \in X$ minimizing the functional $\|u - v\|_V$. In other words, $P_X : V \to X$ is defined as*

$$P_X u := \operatorname*{argmin}_{v \in X} \|u - v\|_V \,.$$

Let $(V, (\cdot,\cdot)_V)$ be a Hilbert space and for $h > 0$ there exists a family of closed subspaces $V_h \subset V$, and $P_h : V \to V_h$ is the orthogonal projection. We are now able to investigate problems of the form

$$\text{find } u \in V : (A + K)u = f, \tag{B.1}$$

and

$$\text{find } u_h \in V_h : P_h(A + K)u_h = P_h f, \tag{B.2}$$

for arbitrary $f \in V$. In this context $K : V \to V$ is a linear, compact operator and $A : V \to V$ a linear, continuous operators for which the solution $u_h \in V_h$ of the projected problem $P_h A u_h = P_h f$ converges for $h \to 0$ to the solution $u \in V$ of $Au = f$.

Theorem B.3. *Let $\Lambda \subset \mathbb{C}$ be an open set, $\hat{\Lambda} \subset \Lambda$ compact, and $A(\lambda) : V \to V$ for $\lambda \in \Lambda$ a family of bounded and linear operators such that the mapping $\lambda \mapsto A(\lambda)$ is continuous. Furthermore, let $K : V \to V$ be a compact operator and there exists a constant $\alpha > 0$ such that for all $\lambda \in \hat{\Lambda}$ there holds $\left|(A(\lambda)v, v)_V\right| \geq \alpha \|v\|^2$ for all $v \in V$.*

Let $V_h \subset V$ with $h > 0$ be a family of closed subspaces of V such that the orthogonal projection $P : V \to V_h$ converges pointwise for $h \to 0$ to the identity $I : V \to V$.

Then $S(\lambda) \coloneqq A(\lambda) + K$ is invertible for all $\lambda \in \hat{\Lambda}$ and there exists $h_0 > 0$, such that $S_h \coloneqq P_h S \colon V_h \to V_h$ is invertible for all $h \leq h_0$ and

$$\sup_{\lambda \in \hat{\Lambda}} \left\| S_h(\lambda)^{-1} \right\| \leq C,$$

for some constant $C > 0$ independent of h.

Proof. See [Nan16]. □

Theorem B.4. *(Generalized Céa) Assume the requirements of the previous theorem hold for $\hat{\Lambda} = \{ \lambda \}$. In particular $S = A + K$ is invertible and $u \in V$ is the unique solution to (B.1). Then there exists $h_0 > 0$, such that (B.2) has a unique solution for all $h \leq h_0$ and there exists a constant $C > 0$ independent of h such that*

$$\|u - u_h\| \leq C \inf_{v_h \in V_h} \|u - v_h\| .$$

Proof. See [Nan16]. □

The previous theorem allows to draw conclusions if $S(\lambda) = A(\lambda) + K$ is invertible. For all remaining cases we explore solutions to eigenvalue problems.

Definition B.5. *(Eigenpairs of nonlinear operators) The pair $(\lambda, u) \in \Lambda \times V \setminus \{ 0 \}$ is an eigenpair of S if and only if*

$$S(\lambda)u = 0.$$

If $s(\cdot,\cdot) = a(\cdot,\cdot) - \lambda b(\cdot,\cdot)$ is composed of sesquilinear forms a, b on $V \times V$, then we can associate operators $A, B \colon V \to V$ and the operator equation $S(\lambda) \coloneqq A - \lambda B$. The discrete eigenvalues problems:

$$\text{Find } (\lambda_h, u_h) \in \mathbb{C} \times V_h \setminus \{ 0 \} : a(u_h, v) = \lambda_h b(u_h, v), \quad v \in V_h, \tag{B.3}$$

are equivalent to the projected problems:

$$\text{Find } (\lambda_h, u_h) \in \mathbb{C} \times V_h \setminus \{ 0 \} : P_h S(\lambda_h) u_h = 0. \tag{B.4}$$

The following theorems operate under the assumption that there exists a discrete set $\Sigma \subset \Lambda$ with no limit point in Λ such that $S(\lambda) = A(\lambda) + K$ is invertible for all $\lambda \in \Lambda \setminus \Sigma$.

Theorem B.6. *Let $(\lambda_h, u_h) \in \Lambda \times V_h \setminus \{ 0 \}$ be a sequence of eigenpairs of the discrete eigenvalues problem (B.4) and λ_h converges to some $\lambda_0 \in \Lambda$ for $h \to 0$. Then $\lambda_0 \in \Sigma$, i.e. the limit of a sequence of discrete eigenvalues is always an eigenvalue of the continuous problem.*

Proof. See [Nan16]. □

Theorem B.7. *For all $\lambda_0 \in \Lambda \setminus \Sigma$ there exist constants $h_0, \varepsilon > 0$ such that the set $\{ \lambda \in \Lambda : |\lambda - \lambda_0| < \varepsilon \}$ contains no eigenvalues of the discrete eigenvalue problem (B.4) for all $h \leq h_0$.*

Proof. See [Nan16]. □

Definition B.8. *(Holomorphic operators) Let* $\Lambda \subset \mathbb{C}$ *be an open set and* $S(\lambda)\colon V \to V$ *for* $\lambda \in \Lambda$ *a holomorphic family of operators, i.e. for all* $\lambda_0 \in \Lambda$ *there exists the derivative*

$$S'(\lambda_0) \coloneqq \lim_{\lambda \to \lambda_0} \frac{1}{\lambda - \lambda_0} \left(S(\lambda) - S(\lambda_0) \right),$$

in the norm on $L(V)$*, the space of linear and bounded operators on* V.

Theorem B.9. *In addition to the previous requirements, assume that* $\lambda \mapsto A(\lambda)$ *is holomorphic. Then for any* $\lambda_0 \in \Sigma$ *there exists a sequence of discrete eigenvalues* λ_h *of (B.3) converging to* λ_0.

Proof. See [Nan16]. □

Nomenclature

Complex scaling:

α	Scaling parameter of a complex scaling function, *8*
$\operatorname{crit} x_\gamma$	Critical region of the complex scaled variable x_γ, *8*
τ	Deformation function, *8*
$H^1_\gamma(\mathbb{R})$	Weighted Sobolev space associated with x_γ, *12*
u_γ	Complex scaled function, *8*
x_γ	Complex scaled variable, *8*

General:

$\arg(f(x))$	Complex argument of $f(x)$ in the interval $[-\pi, \pi)$, *9*
$\mathbb{1}_A$	Indicator function of the set A, *10*
$\mathbb{N}_0$	Natural numbers including zero, *10*
$\mathbb{R}_{\geq 0}$	Non-negative real numbers, *7*
$\operatorname{supp} f$	Support of $f : \Omega \to R$. $\operatorname{supp} f \coloneqq \overline{\{\, x \in \Omega : f(x) \neq 0 \,\}}$, *4*
$\operatorname{supp}_\varepsilon f$	Essential support of $f : \Omega \to R$. $\operatorname{supp}_\varepsilon f \coloneqq \overline{\{\, x \in \Omega : \lvert f(x) \rvert \geq \varepsilon \,\}}$, *32*
$B_r(x)$	The open ball of radius r around x, *14*
$H^1_{\mathrm{comp}}(\mathbb{R})$	Subspace of $H^1(\mathbb{R})$ containing all functions with compact support, *4*
$H^1_{\mathrm{loc}}(\mathbb{R})$	Subspace of $H^1(\mathbb{R})$ containing all locally integrable functions, *4*
$L^\infty(\Omega)$	Banach space of essentially bounded functions on Ω, *4*
$W^{m,p}(\Omega)$	Sobolev space (A.1), *45*

List of Figures

Bibliography

[Ber94] J.-P. Berenger. “A Perfectly Matched Layer for the Absorption of Electromagnetic Waves”. In: *Journal of Computational Physics* 114 (Oct. 1994), pp. 185–200. DOI: `10.1006/jcph.1994.1159`.

[Eva10] Lawrence C. Evans. *Partial Differential Equations: Second Edition (Graduate Studies in Mathematics)*. American Mathematical Society, 2010. ISBN: 0821849743.

[Fau09] Markus Faustmann. *Bachelor thesis on Gewichtete Sobolev-Räume und nicht ”klassische“ lineare elliptische Randwertprobleme*. 2009. URL: `https://www.asc.tuwien.ac.at/~arnold/lehre/pdf/weightedSobolev.pdf`.

[HN09] Thorsten Hohage and Lothar Nannen. “Hardy Space Infinite Elements for Scattering and Resonance Problems”. In: *SIAM Journal on Numerical Analysis* 47.2 (Jan. 2009), pp. 972–996. DOI: `10.1137/070708044`. URL: `https://doi.org/10.1137/070708044`.

[HSZ03a] Thorsten Hohage, Frank Schmidt, and Lin Zschiedrich. “Solving Time-Harmonic Scattering Problems Based on the Pole Condition I: Theory”. In: *SIAM Journal on Mathematical Analysis* 35.1 (Jan. 2003), pp. 183–210. DOI: `10.1137/s0036141002406473`. URL: `https://doi.org/10.1137/s0036141002406473`.

[HSZ03b] Thorsten Hohage, Frank Schmidt, and Lin Zschiedrich. “Solving Time-Harmonic Scattering Problems Based on the Pole Condition II: Convergence of the PML Method”. In: *SIAM Journal on Mathematical Analysis* 35.3 (Jan. 2003), pp. 547–560. DOI: `10.1137/s0036141002406485`. URL: `https://doi.org/10.1137/s0036141002406485`.

[Jän11] Klaus Jänich. *Funktionentheorie: Eine Einführung (Springer-Lehrbuch) (German Edition)*. Springer, 2011. ISBN: 3540203923.

[Jün17] Ansgar Jüngel. *Lecture notes in Partielle Differentialgleichungen*. Dec. 2017. URL: `https://www.asc.tuwien.ac.at/~juengel/scripts/PDE.pdf`.

[Kre02] R. Kress. “Specific Theoretical Tools”. In: *Scattering*. Elsevier, 2002, pp. 37–51. DOI: `10.1016/b978-012613760-6/50004-8`. URL: `https://doi.org/10.1016/b978-012613760-6/50004-8`.

[Kre99] Raimer Kress. *Linear Integral Equations (Applied Mathematical Sciences) (Vol 82)*. Springer, 1999. ISBN: 0387987002.

[Kuf84] Opic Kufner. “How to define reasonably weighted Sobolev spaces”. eng. In: *Commentationes Mathematicae Universitatis Carolinae* 025.3 (1984), pp. 537–554. URL: `http://eudml.org/doc/17341`.

[Nan16] Lothar Nannen. *Lecture notes in Streu- und Resonanzprobleme*. June 2016. URL: http://www.asc.tuwien.ac.at/~lnannen/Lectures/Scattering2016/ScatteringProblems.pdf.

[Nol08] Wolfgang Nolting. *Grundkurs Theoretische Physik 5/1: Quantenmechanik - Grundlagen (Springer-Lehrbuch) (German Edition)*. Springer, 2008. ISBN: 3540688684.

[NW18] Lothar Nannen and Markus Wess. “Computing scattering resonances using perfectly matched layers with frequency dependent scaling functions”. In: *BIT Numerical Mathematics* 58.2 (June 2018), pp. 373–395. ISSN: 1572-9125. DOI: 10.1007/s10543-018-0694-0. URL: https://doi.org/10.1007/s10543-018-0694-0.

[Sch09] Joachim Schöberl. *Lecture notes in Numerical Methods for Partial Differential Equations*. Apr. 2009. URL: http://www.asc.tuwien.ac.at/~schoeberl/wiki/lva/notes/numpde.pdf.

[Sch14] Joachim Schöberl. *C++11 Implementation of Finite Elements in NGSolve*. Sept. 2014.